STEVENS
Institute of Technology

New Developments in Simulation and Modeling of the Twin Screw Extrusion Process

Dilhan Kalyon/Moinuddin Malik

HfMI

Stevens Institute of Technology

Fig. 1

STEVENS Institute of Technology

- For Energetics there is very little room for experimentation and trial and error in continuous processing of solid rocket fuels, propellants, explosives; process is not forgiving
- Wrong marriage of conditions, geometry and material properties will result in an incident
- Energetic materials are complex structured fluids with degrees of high solid fill (50-88% by volume).

Fig. 2

STEVENS Institute of Technology

Continuous processing of such complex fluids at minimum or no trial and error requires

- Apriori characterization of the rheological behavior of the energetic formulation
- Mathematical modeling of the process
- Good understanding of the structure development aspects
- Ways of characterization of microstructural distributions and understanding of structure/rheology relationships
- Methods to verify-Validate

Fig. 3

STEVENS Institute of Technology

Methodology:

- Step #1: Determine the constraints (maximum temperature, residence time, stress magnitude, binder/particle migration/air…..)
- Step #2: Characterize rheological behavior as a function of specific energy input concomitant with documentation of microstructural distributions

Fig. 4

STEVENS Institute of Technology

Methodology:

- Step #3: Determine which type of continuous processor satisfies the constraints (single or twin, co versus counter, tangential versus fully-intermeshing)
- Step #4: Determine typical screw/barrel configuration and operating conditions

Fig. 5

STEVENS Institute of Technology

Methodology:

- Step #5: Verify all at lab scale using well-instrumented machines (simulation versus experiment, rheological behavior, structure…)
- Step #6: Design and build additional hardware necessary for the manufacturing operation (dies…)
- Step #7: Test all at manufacturing scale (simulation versus experiment, rheological behavior, structure…)

Fig. 6

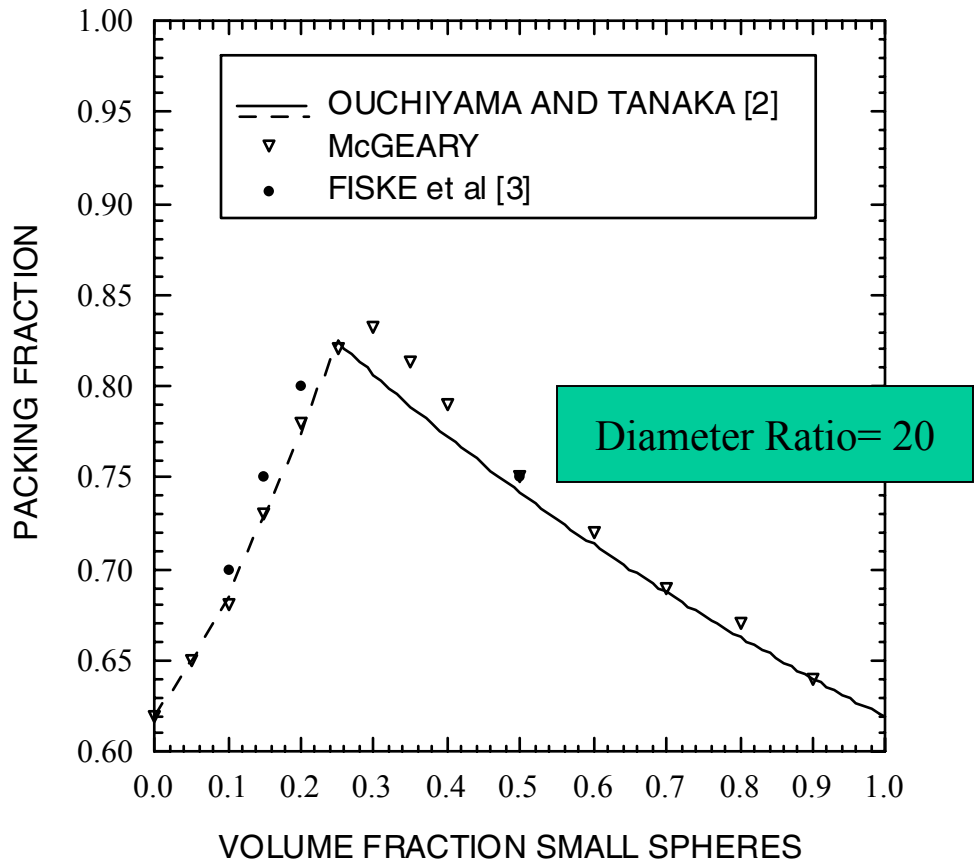

Major challenge arises from the highly filled nature of the energetic materials, need to work at particle volume loading levels which approach the maximum packing fraction

Fig. 7

STEVENS Institute of Technology

Challenges: Rheology

- Wall slip associated with all highly filled materials; energetics have very high degrees of solid fill
- Viscoplasticity
- Ease of separation of the binder from the solids
- Complex microstructural distributions, which are affected by the thermo-mechanical history during processing

Fig. 8

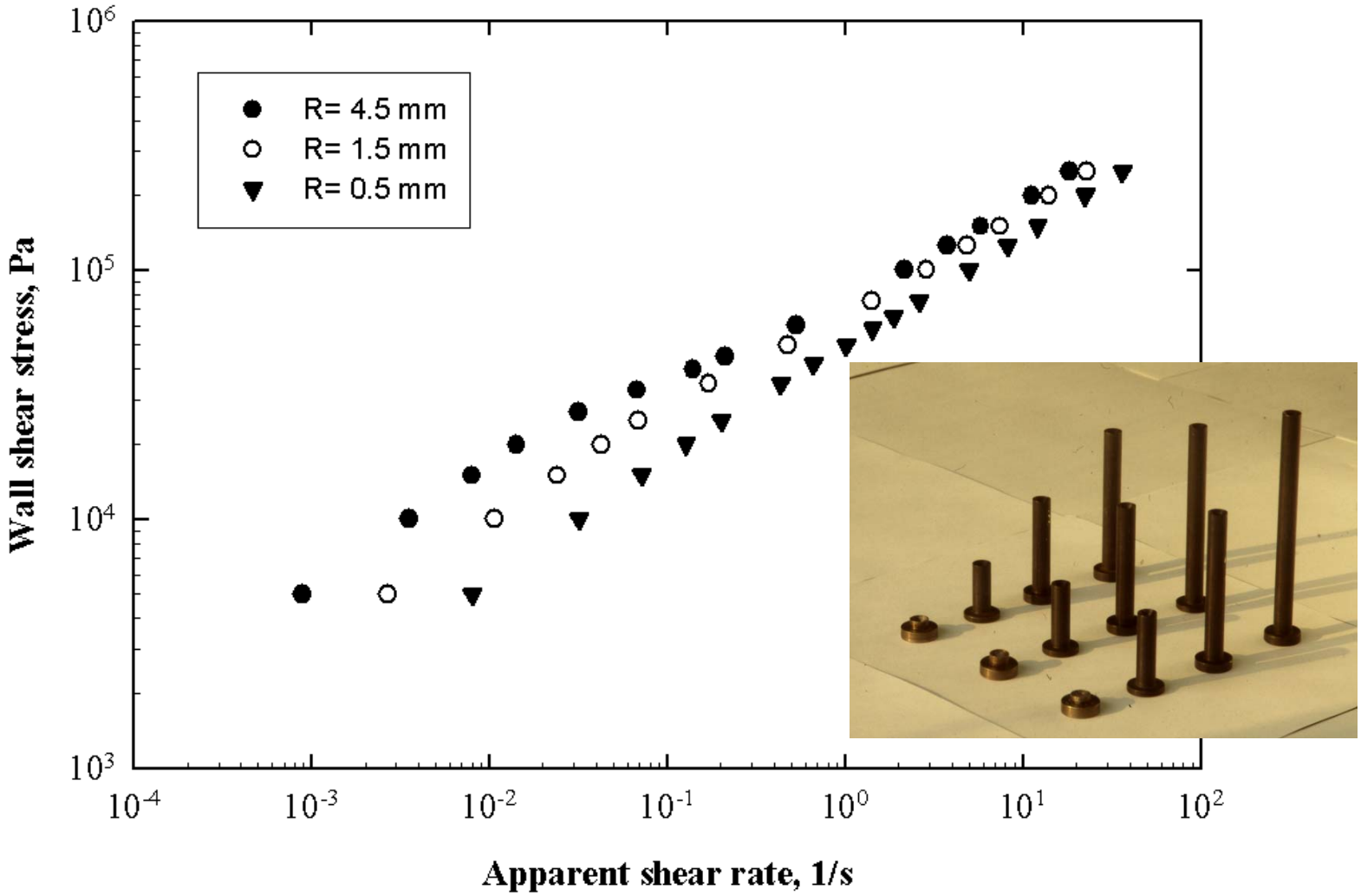
R= 4.5 mm
R= 1.5 mm
R= 0.5 mm
Wall shear stress, Pa
Apparent shear rate, 1/s
10^6
10^5
10^4
10^3
10^{-4}
10^{-3}
10^{-2}
10^{-1}
10^0
10^1
10^2

Fig. 9

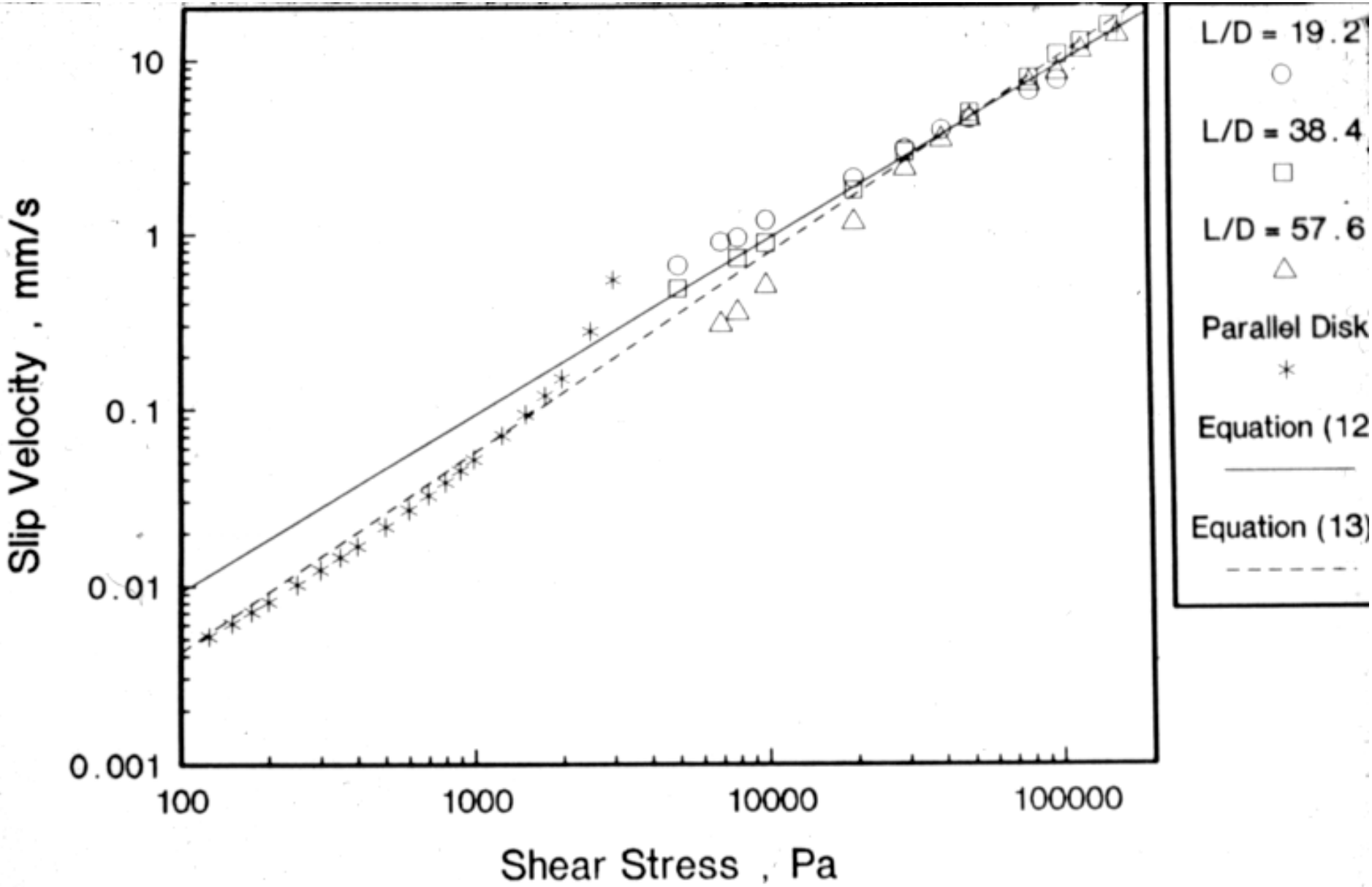

Figure 5

Fig. 10

- Occurs on the basis of the formation of a particle-free apparent slip layer (Vand Layer)
- Alters apparent rheological behavior
- Needs to be incorporated into simulation as the wall boundary condition (Navier's slip condition)

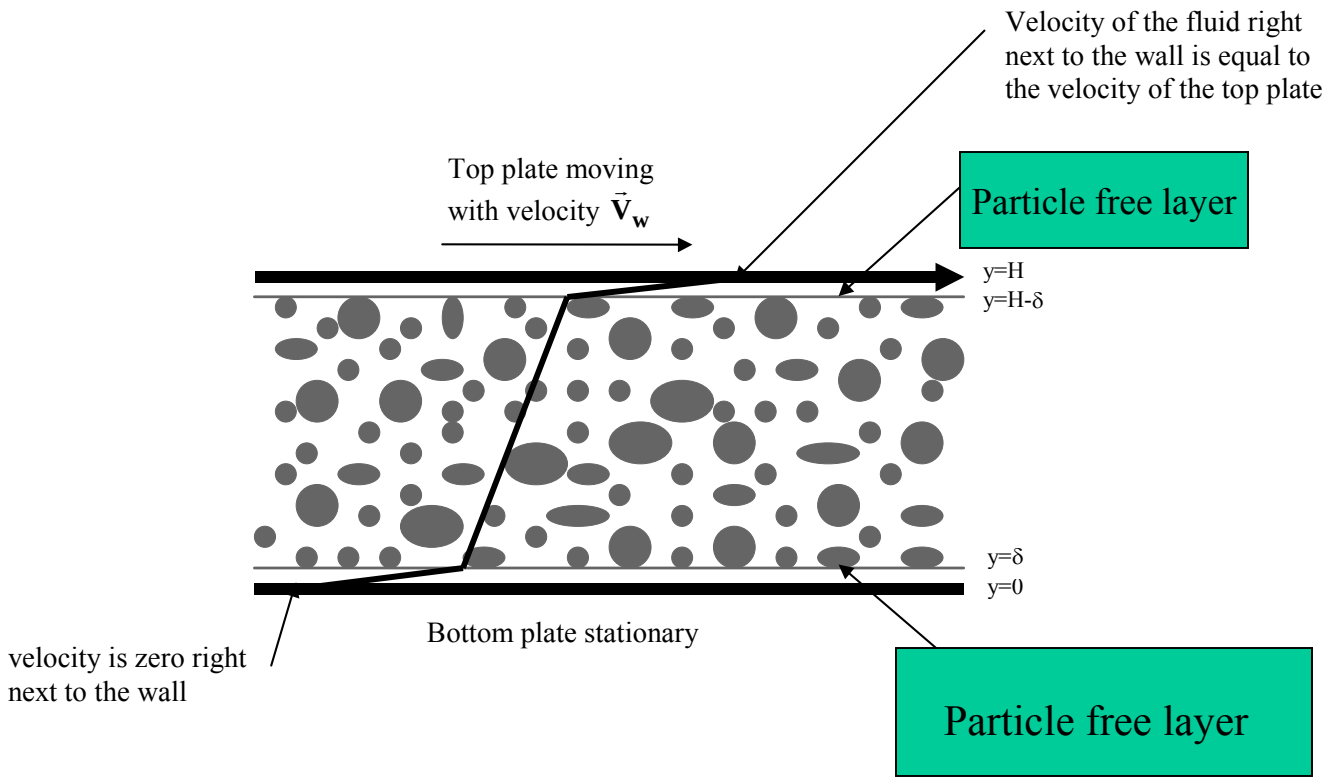

Fig. 11

wall slip in filled polymers

b.

a.

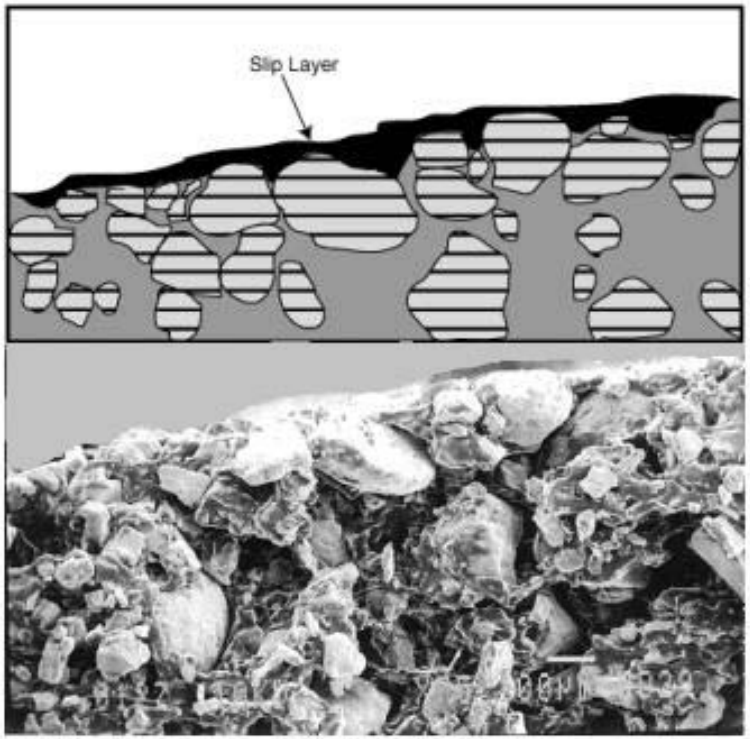

Fig. 12

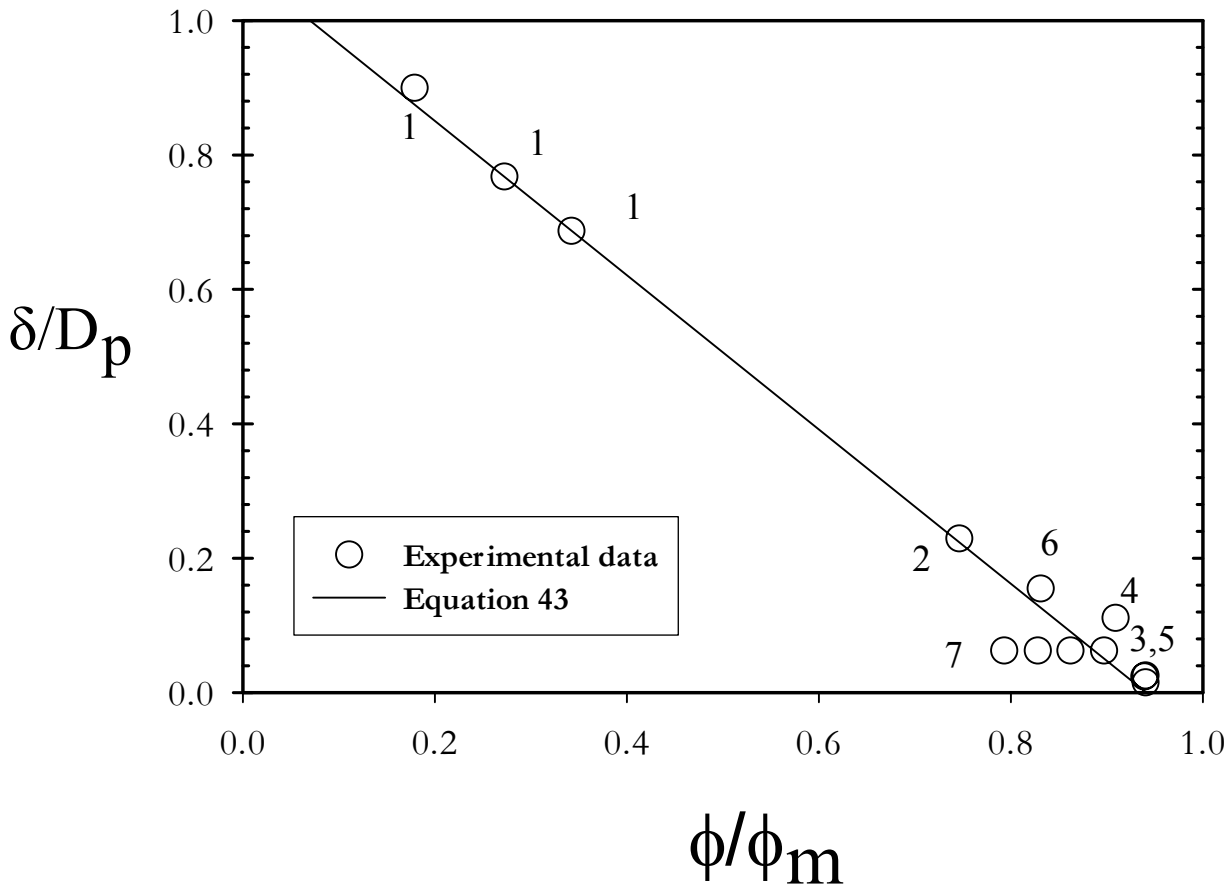
1.0
0.8
0.6
0.4
0.2
0.0
δ/Dp
0.0
0.2
0.4
0.6
0.8
1.0
ϕ/ϕm
Experimental data
Equation 43
1
1
1
2
6
4
3,5
7

Fig. 13

Slip velocity, Us, versus wall shear stress, τw

$$U_s = \beta \tau_w{}^{sb}$$

β= f(apparent slip layer thickness, d, binder shear viscosity)
sb=f (binder shear viscosity)

Fig. 14

Specialized rheometers are necessary

- Better to load the rheometer under vacuum (best with remote loading capability)
- Need to change the surface to volume ratio of the rheometer continuously to characterize wall slip and yielding effects
- Need to follow the structure formation and segregation aspects during characterization

Fig. 15

Concentrated suspensions are structured complex fluids

- The binder can segregate out of the suspension under certain conditions
- The particles may migrate in the transverse to flow direction generating concentration gradients
- The amount of specific energy input during the mixing alters the structure and the rheology of the formulation
- The air incorporated during the process alters the rheology and the processability of the energetic material.
- The size distribution of the particles can change during the process.

Fig. 16

Need to characterize and then use as part of the constraints:

- Conditions under which the binder separates from the particles (jamming/demixing)
- Conditions under which the particles migrate to generate significant concentration gradients
- Flow instabilities/extrudate distortions
- Any changes in structure (degradation, air incorporation, changes in particle size….)

Fig. 17

UPON FILTRATION OF THE BINDER THE REMAINDER IS SOLID-LIKE

The Grinding of the Powder in the Extruder upon the Filtration of the Binder and Mat Formation

∅=0.765

Ammonium sulfate into the extruder

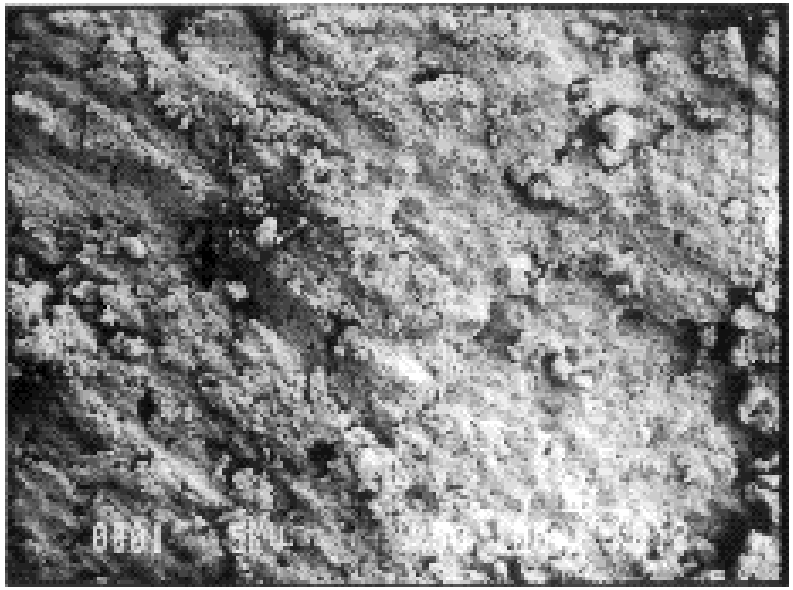

Ammonium sulfate ground in the extruder (same scale)

Fig. 18

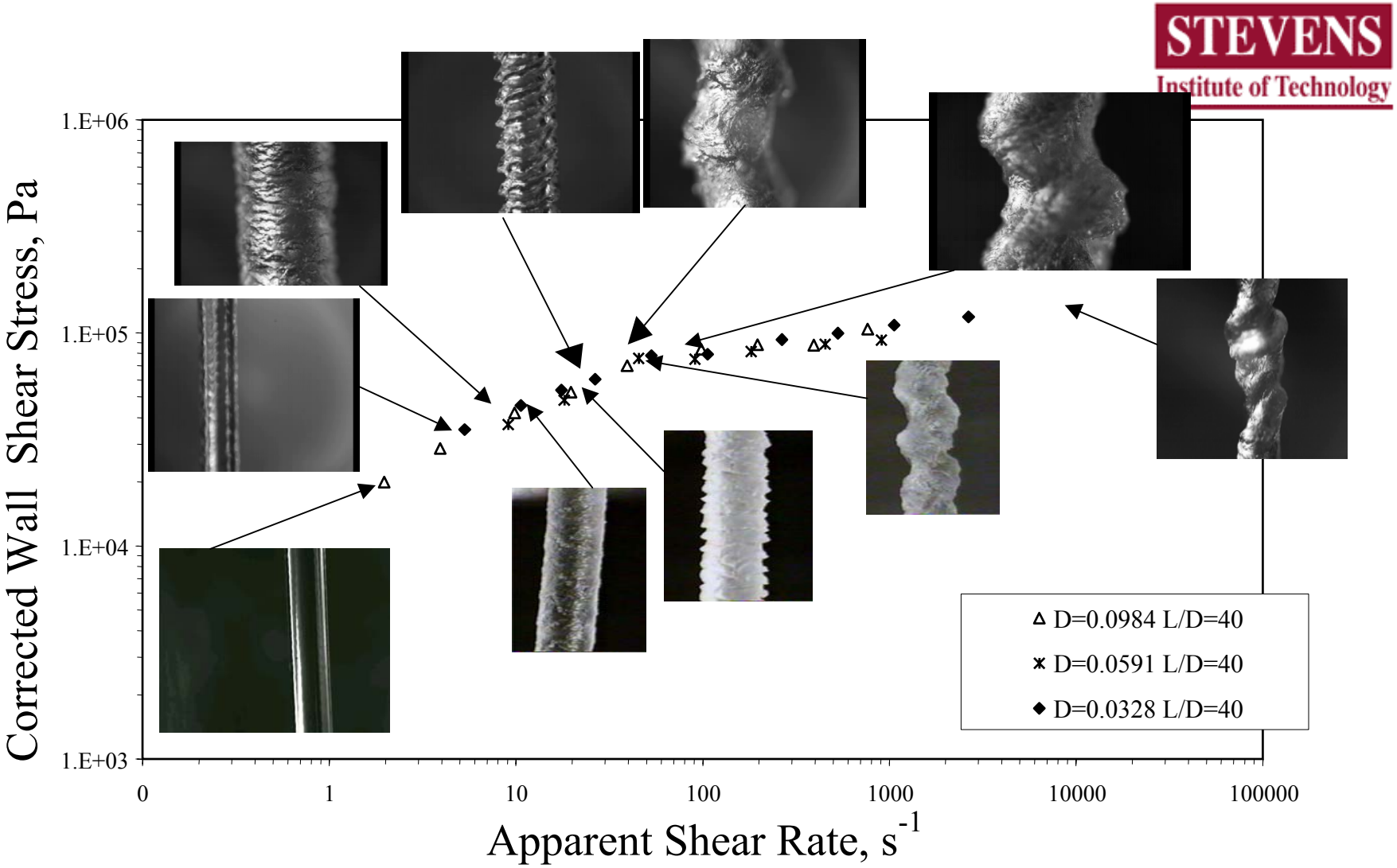

Conditions for the onset of flow instabilities and extrudate distortions

Fig. 19

Shear-induced Migration in Poiseuille Flow

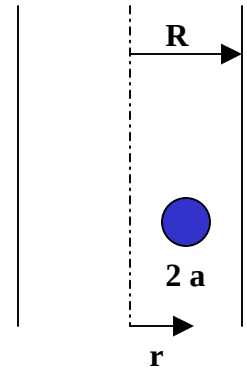

- Shear-induced Migration Model
  - Phillips et al. (1992)

$$v_z \frac{\partial \phi}{\partial z} = \frac{a^2}{r} \frac{\partial}{\partial r} \left\{ r \left[K_c \left(\phi^2 \frac{\partial \dot{\gamma}}{\partial r} + \dot{\gamma} \phi \frac{\partial \phi}{\partial r} \right) + K_\eta \frac{\dot{\gamma} \phi^2}{\eta_s} \frac{\partial \eta_s}{\partial r} \right] \right\}$$

- Boundary Conditions
  - Total Particle Flux at Tube Wall

$$K_c \phi \left(\phi \frac{\partial \dot{\gamma}}{\partial r} + \dot{\gamma} \frac{\partial \phi}{\partial r} \right) + K_\eta \frac{\dot{\gamma} \phi^2}{\eta_s} \frac{\partial \eta_s}{\partial r} = 0 \qquad r = R$$

  - Symmetry Condition at Axis of Symmetry

$$\frac{\partial \phi}{\partial r} = 0 \qquad r = 0$$

Fig. 20

Concentration Distribution in Poiseuille Flow

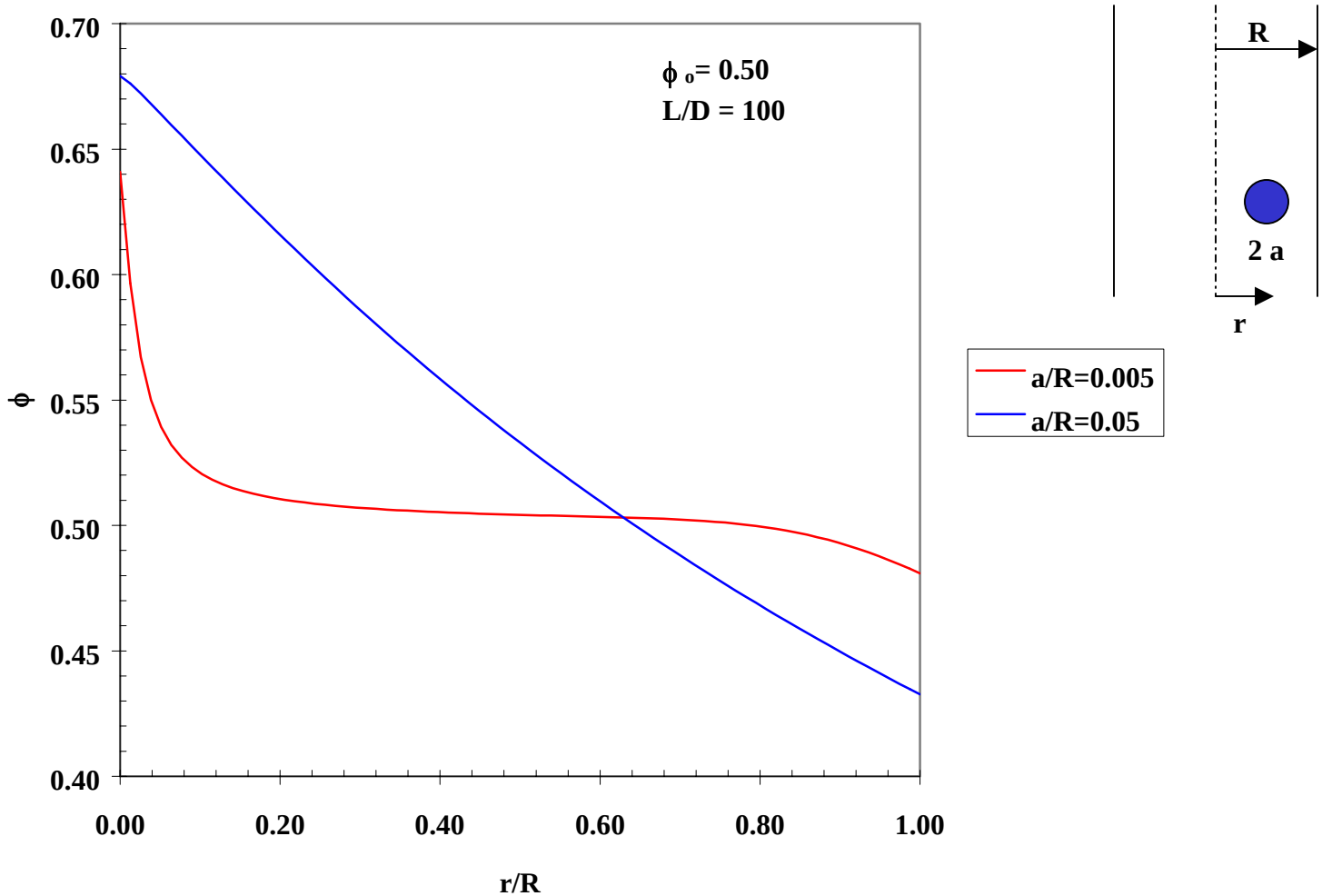

Fig. 21

Modeling is necessary to optimize extruder selection, geometry and operating conditions

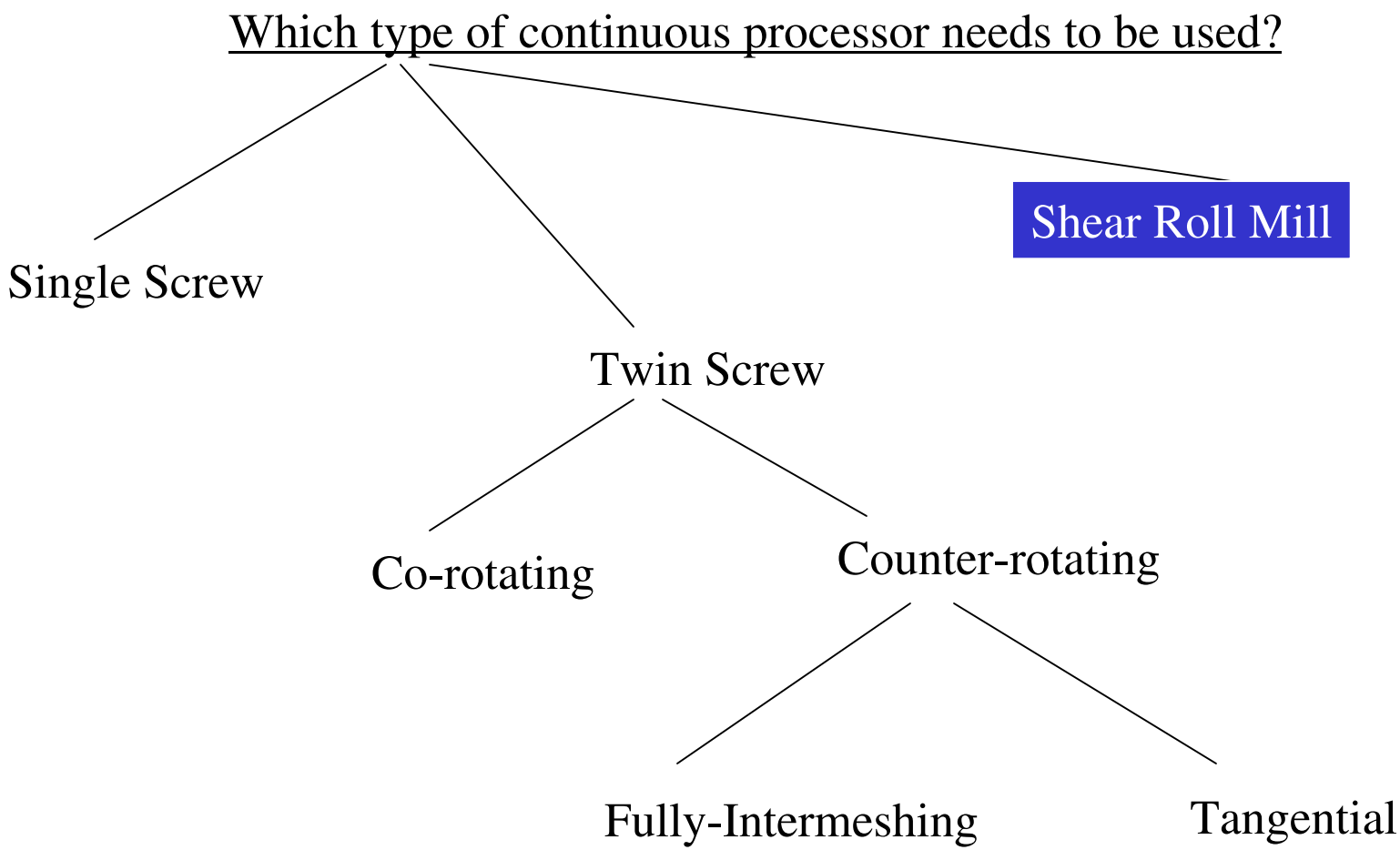

Fig. 22

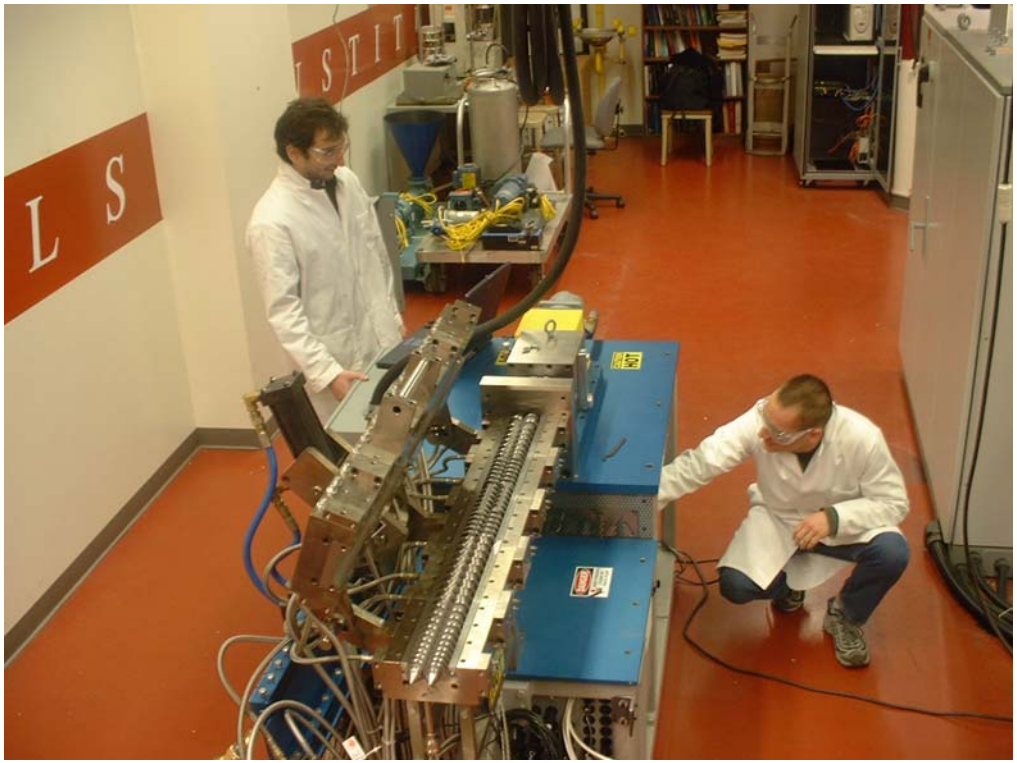

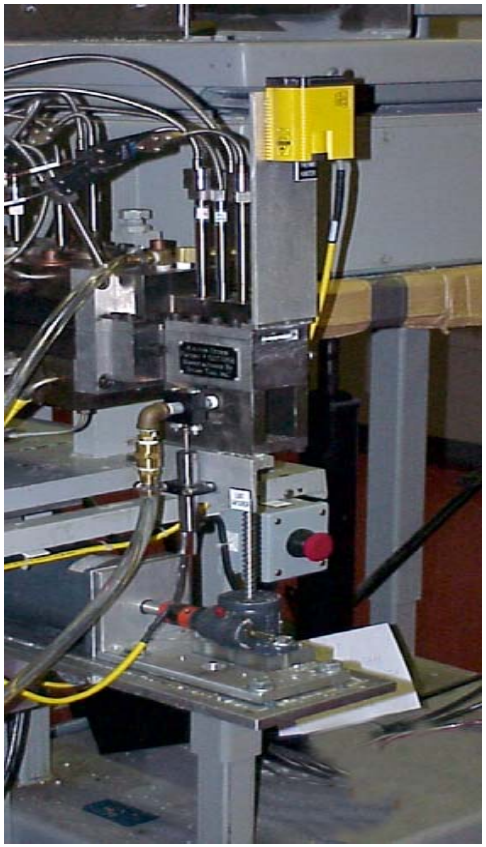

Universal extrusion system for energetics
*Co-rotating
*Counter-rotating tangential
*Counter-rotating fully-intermeshing
*Single screw extruder

Adjustable gap rheometer

Fig. 23

Conservation equations

$$\frac{\partial u}{\partial x}+\frac{\partial v}{\partial y}+\frac{\partial w}{\partial z}=0$$

$$\frac{\partial}{\partial x}(2\eta\frac{\partial u}{\partial x})+\frac{\partial}{\partial y}\{\eta(\frac{\partial u}{\partial y}+\frac{\partial v}{\partial x})\}+\frac{\partial}{\partial z}\{\eta(\frac{\partial u}{\partial z}+\frac{\partial w}{\partial x})\}-\frac{\partial p}{\partial x}=0$$

$$\frac{\partial}{\partial x}\{\eta(\frac{\partial v}{\partial x}+\frac{\partial u}{\partial y})\}+\frac{\partial}{\partial y}(2\eta\frac{\partial v}{\partial y})+\frac{\partial}{\partial z}\{\eta(\frac{\partial v}{\partial z}+\frac{\partial w}{\partial y})\}-\frac{\partial p}{\partial y}=0$$

$$\frac{\partial}{\partial x}\{\eta(\frac{\partial w}{\partial x}+\frac{\partial u}{\partial z})\}+\frac{\partial}{\partial y}\{\eta(\frac{\partial w}{\partial y}+\frac{\partial v}{\partial z})\}+\frac{\partial}{\partial z}(2\eta\frac{\partial w}{\partial z})-\frac{\partial p}{\partial z}=0$$

$$\rho C_p(u\frac{\partial T}{\partial x}+v\frac{\partial T}{\partial y}+w\frac{\partial T}{\partial z})-k(\frac{\partial^2 T}{\partial x^2}+\frac{\partial^2 T}{\partial y^2}+\frac{\partial^2 T}{\partial z^2})-\eta\,|\dot{\gamma}|^2=0$$

Fig. 24

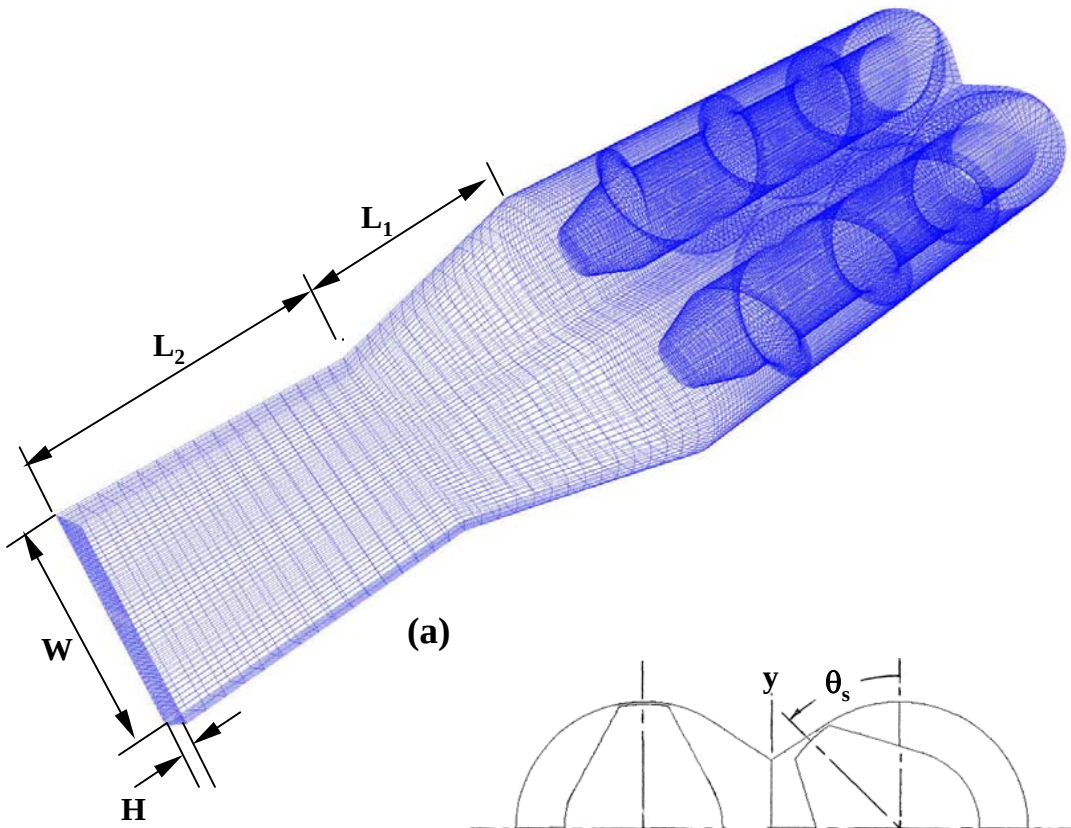

(a)

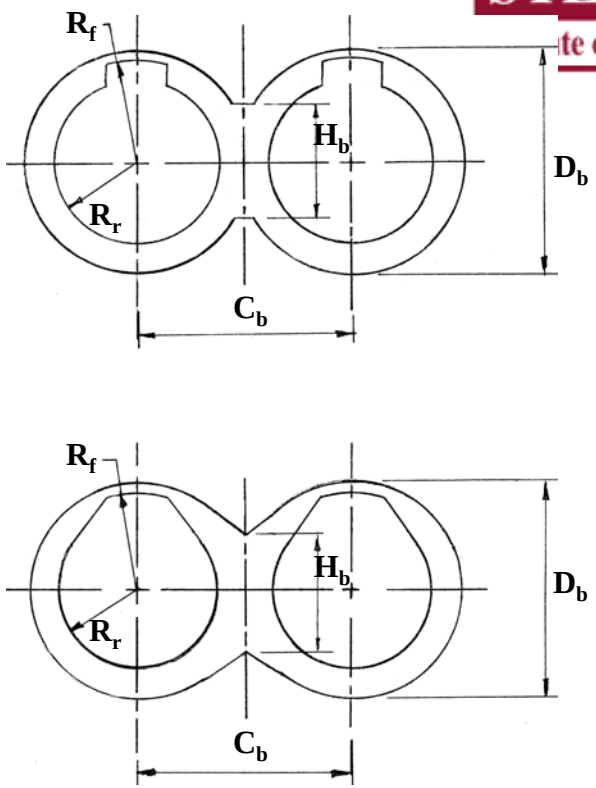

(b)

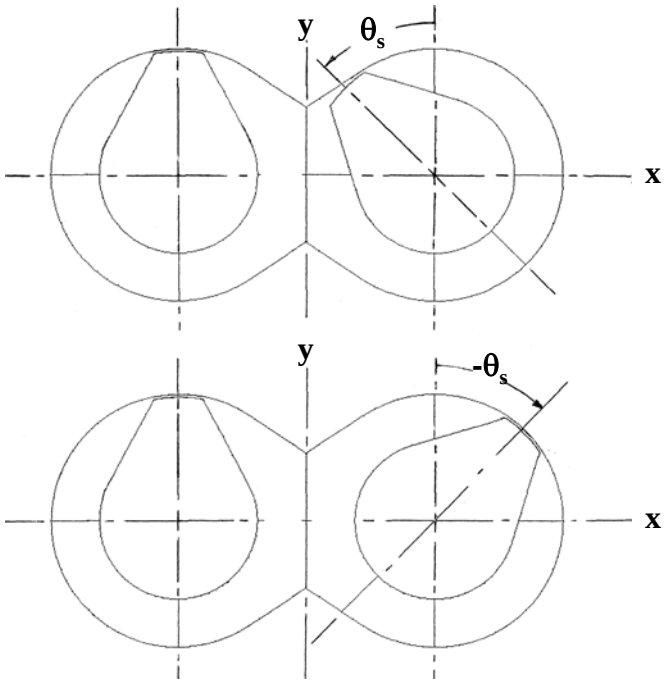

(c)

Counter tangential

Fig. 25

Counter tangential

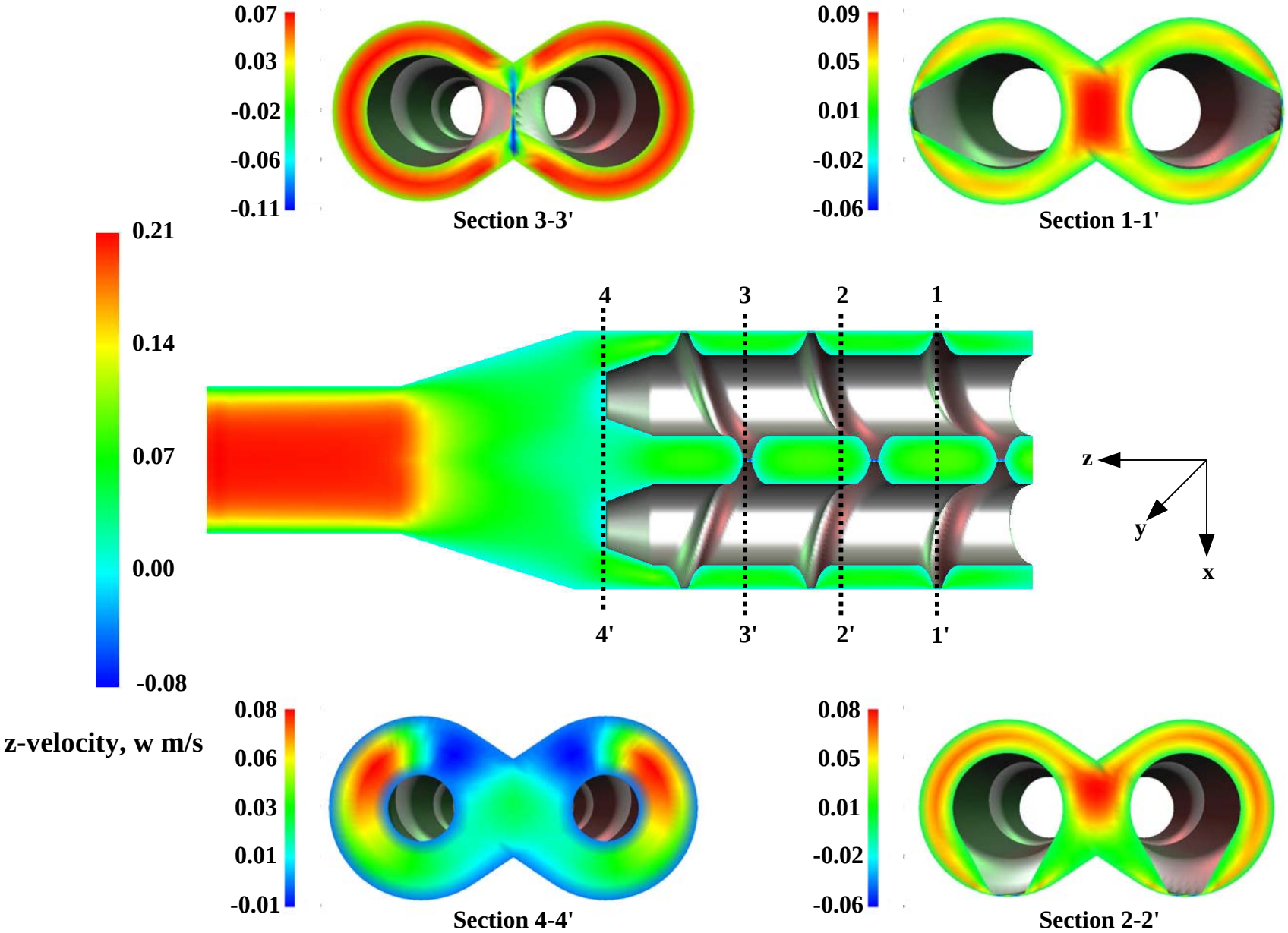

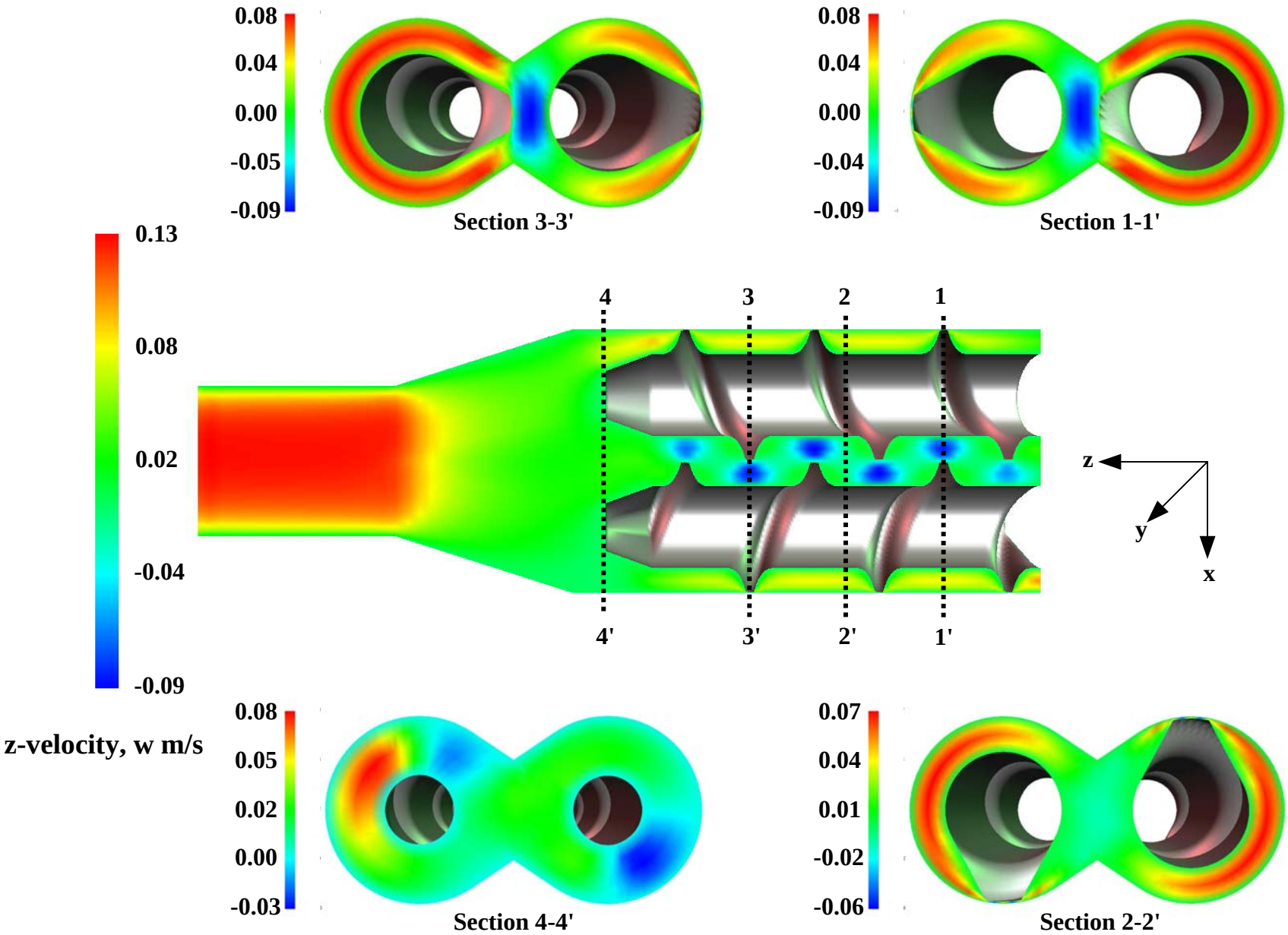
0.08
0.04
0.00
-0.05
-0.09
Section 3-3'
0.08
0.04
0.00
-0.04
-0.09
Section 1-1'
0.13
0.08
0.02
-0.04
-0.09
z-velocity, w m/s
4
3
2
1
4'
3'
2'
1'
z
y
x
0.08
0.05
0.02
0.00
-0.03
Section 4-4'
0.07
0.04
0.01
-0.02
-0.06
Section 2-2'

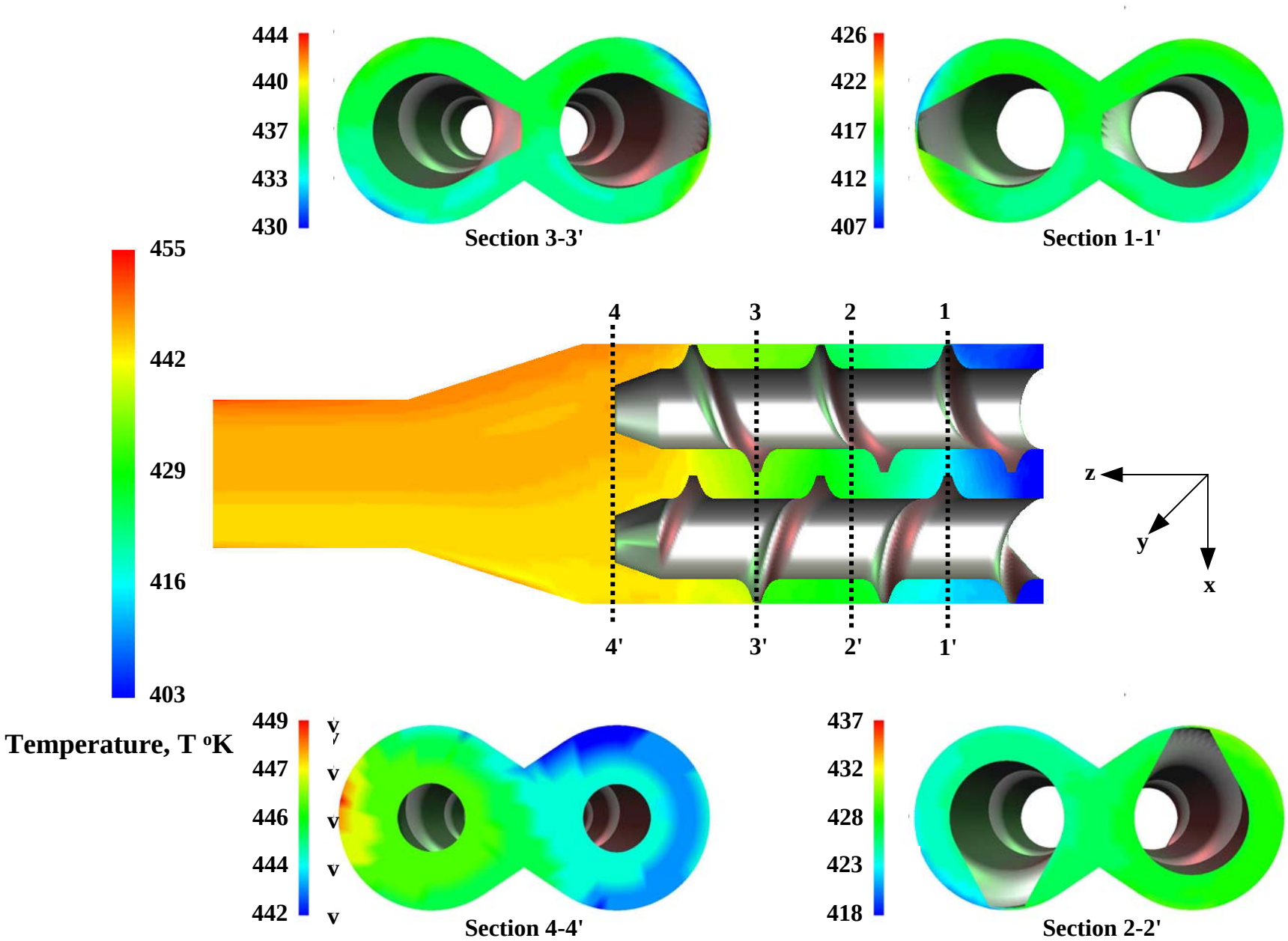
444
440
437
433
430
Section 3-3'
426
422
417
412
407
Section 1-1'
455
442
429
416
403
Temperature, T °K
4
3
2
1
4'
3'
2'
1'
z
y
x
449
447
446
444
442
Section 4-4'
437
432
428
423
418
Section 2-2'

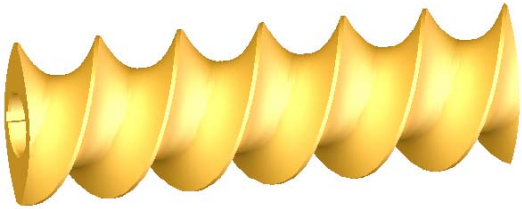

Forward

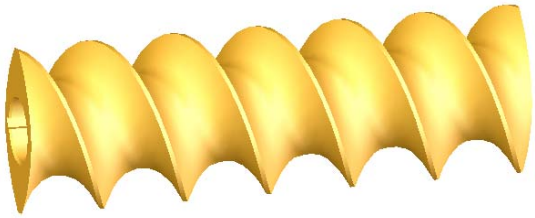

Reverse

Fully flighted forward and reverse screw elements

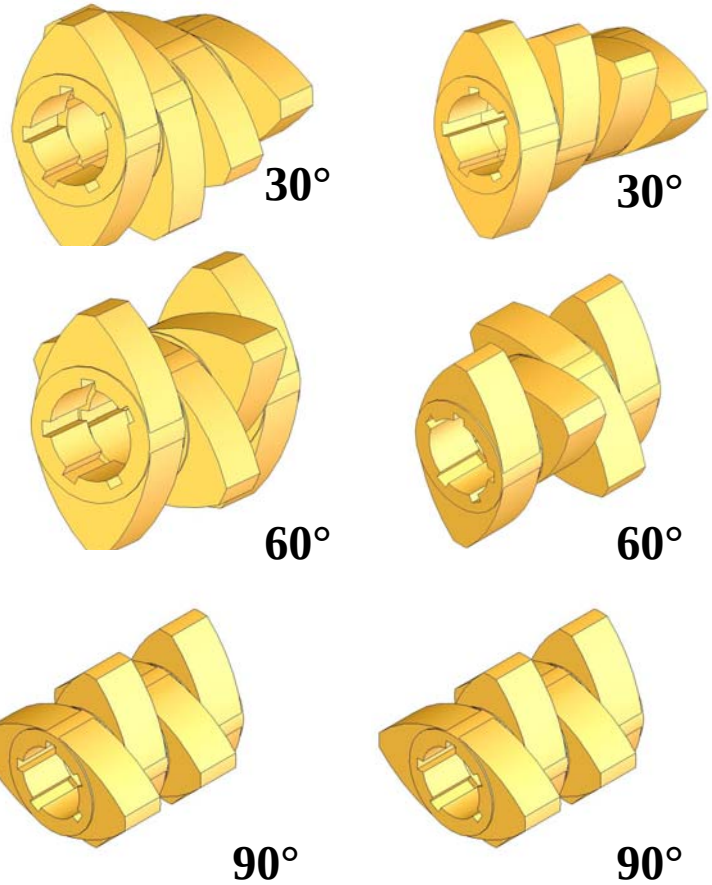

Forward 30, 60, 90 ° kneading blocks

Reverse 30, 60, 90 ° kneading blocks

Fig. 29

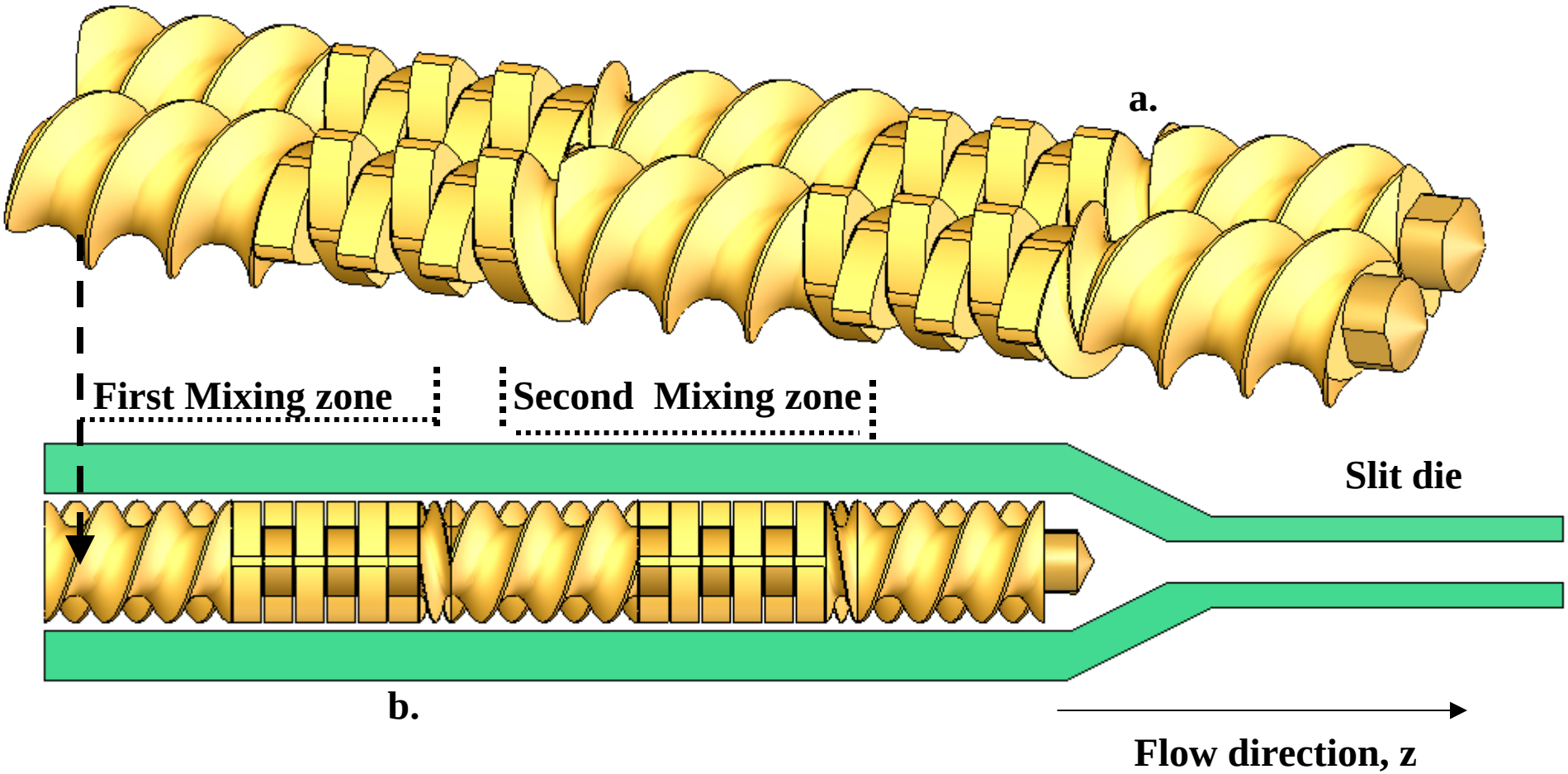
a.
First Mixing zone
Second Mixing zone
Slit die
b.
Flow direction, z

Fig. 30

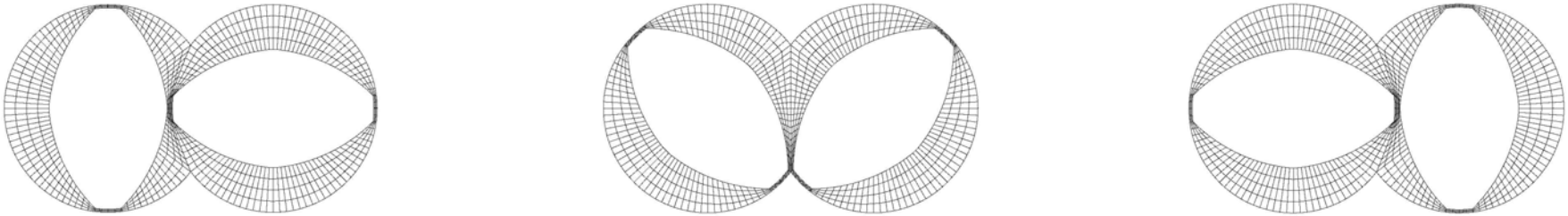

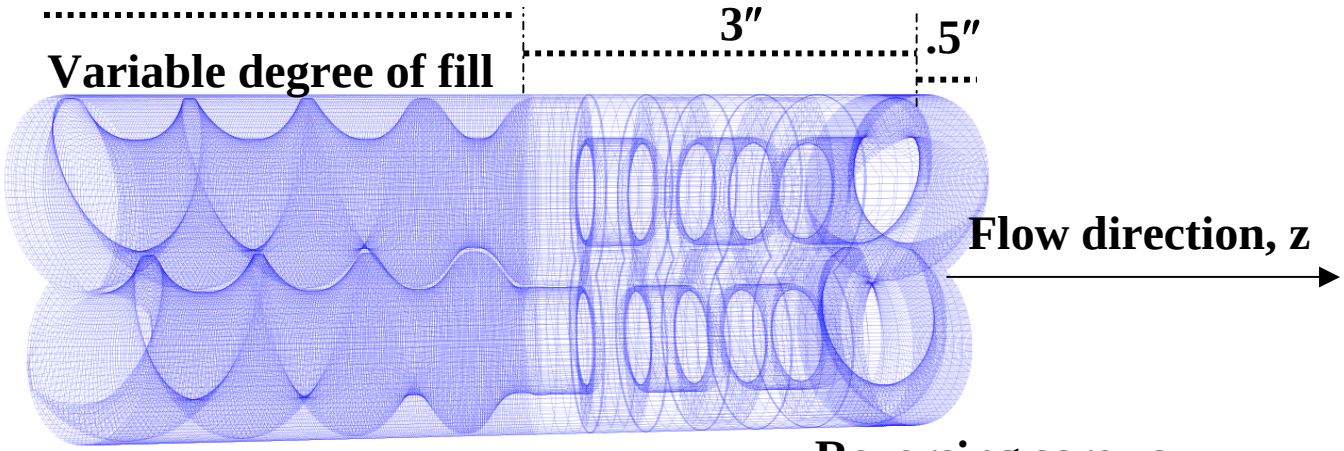
3″
.5″
Variable degree of fill
Flow direction, z
Reversing screws

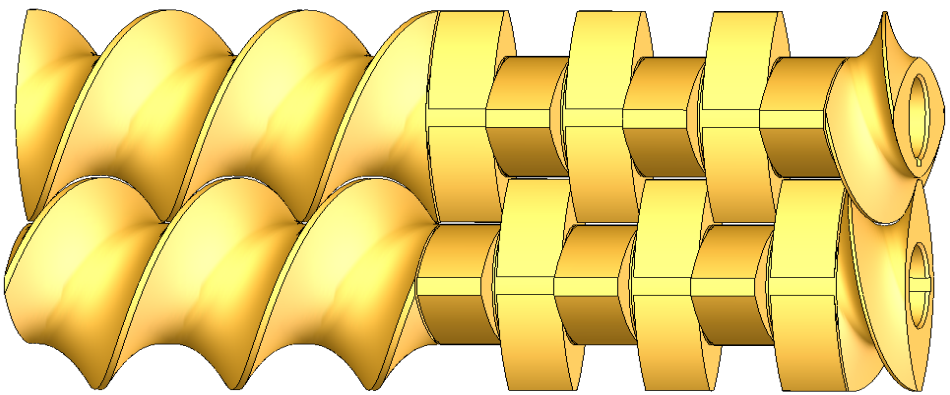
Forwarding fully-flighted screws
Kneading discs

Fig. 31

Co-rotating twin screw extruder: same die: adjustable gap slit rheometer

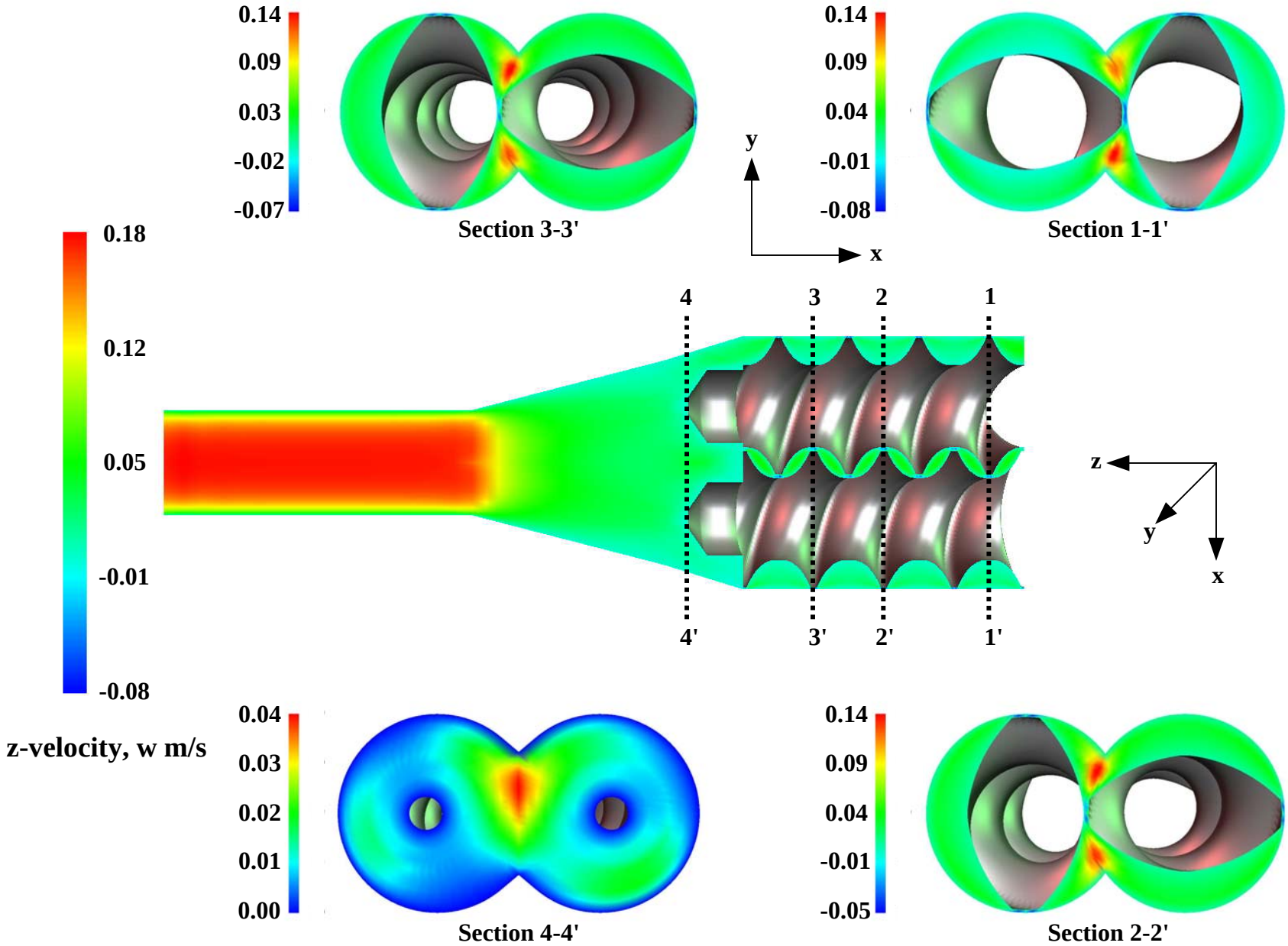

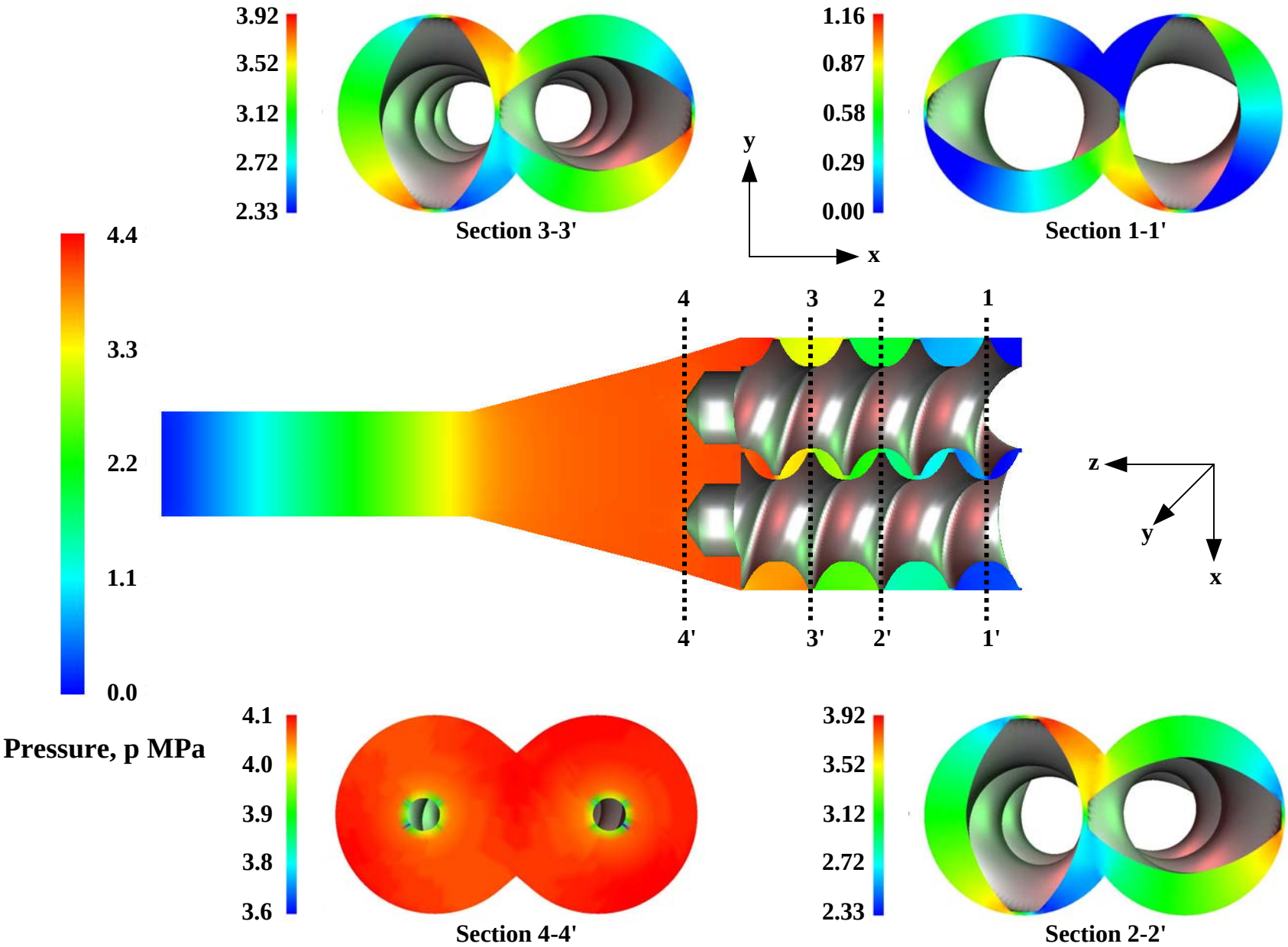
3.92
3.52
3.12
2.72
2.33
Section 3-3'
1.16
0.87
0.58
0.29
0.00
Section 1-1'
y
x
4.4
3.3
2.2
1.1
0.0
Pressure, p MPa
4
3
2
1
4'
3'
2'
1'
z
y
x
4.1
4.0
3.9
3.8
3.6
Section 4-4'
3.92
3.52
3.12
2.72
2.33
Section 2-2'

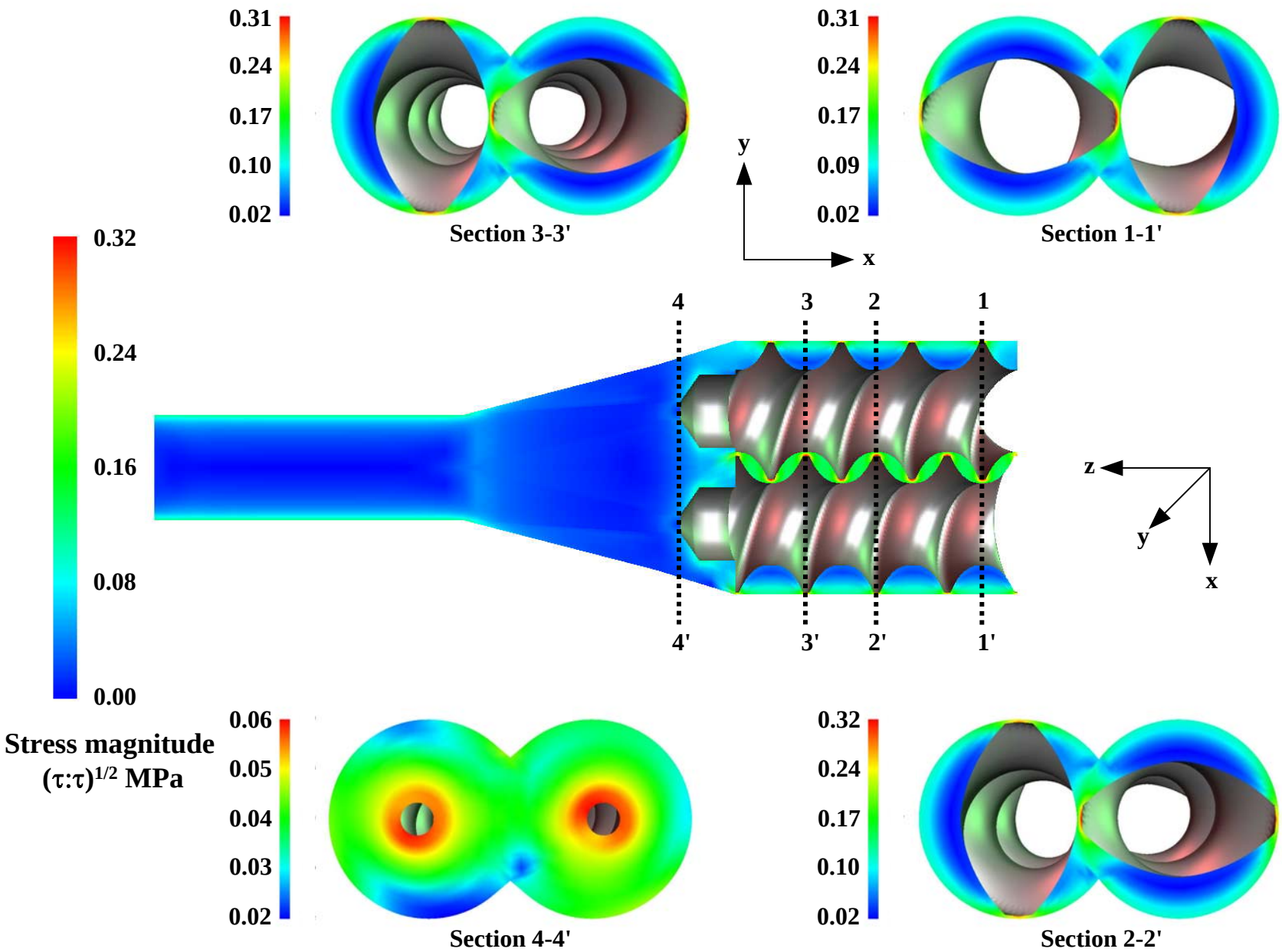
0.31
0.24
0.17
0.10
0.02
Section 3-3'
y
x
0.31
0.24
0.17
0.09
0.02
Section 1-1'
0.32
0.24
0.16
0.08
0.00
Stress magnitude
(τ:τ)^1/2 MPa
4
3
2
1
4'
3'
2'
1'
z
y
x
0.06
0.05
0.04
0.03
0.02
Section 4-4'
0.32
0.24
0.17
0.10
0.02
Section 2-2'

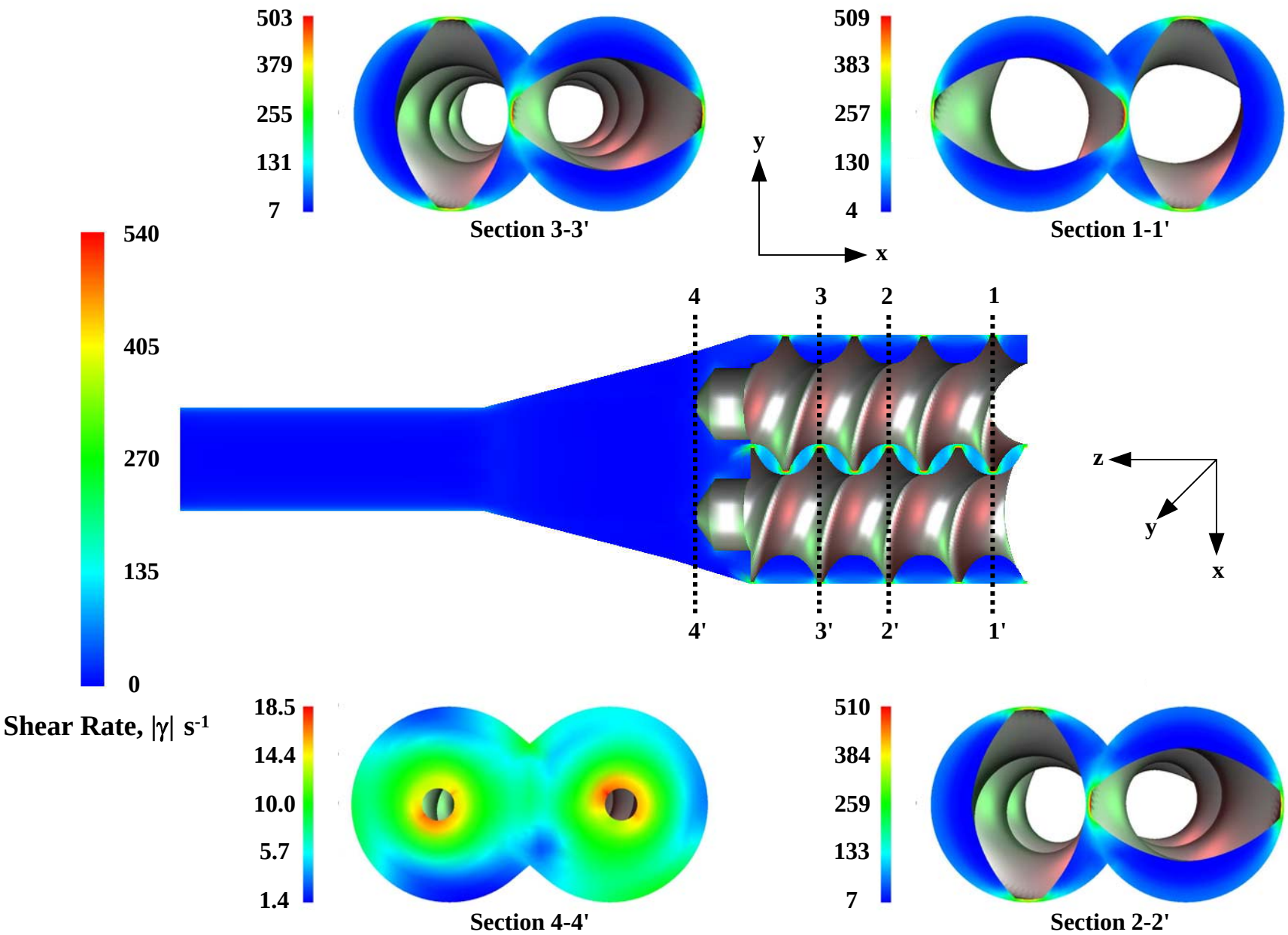
503
379
255
131
7
Section 3-3'
509
383
257
130
4
Section 1-1'
y
x
540
405
270
135
0
Shear Rate, |γ| s-1
4
3
2
1
4'
3'
2'
1'
z
y
x
18.5
14.4
10.0
5.7
1.4
Section 4-4'
510
384
259
133
7
Section 2-2'

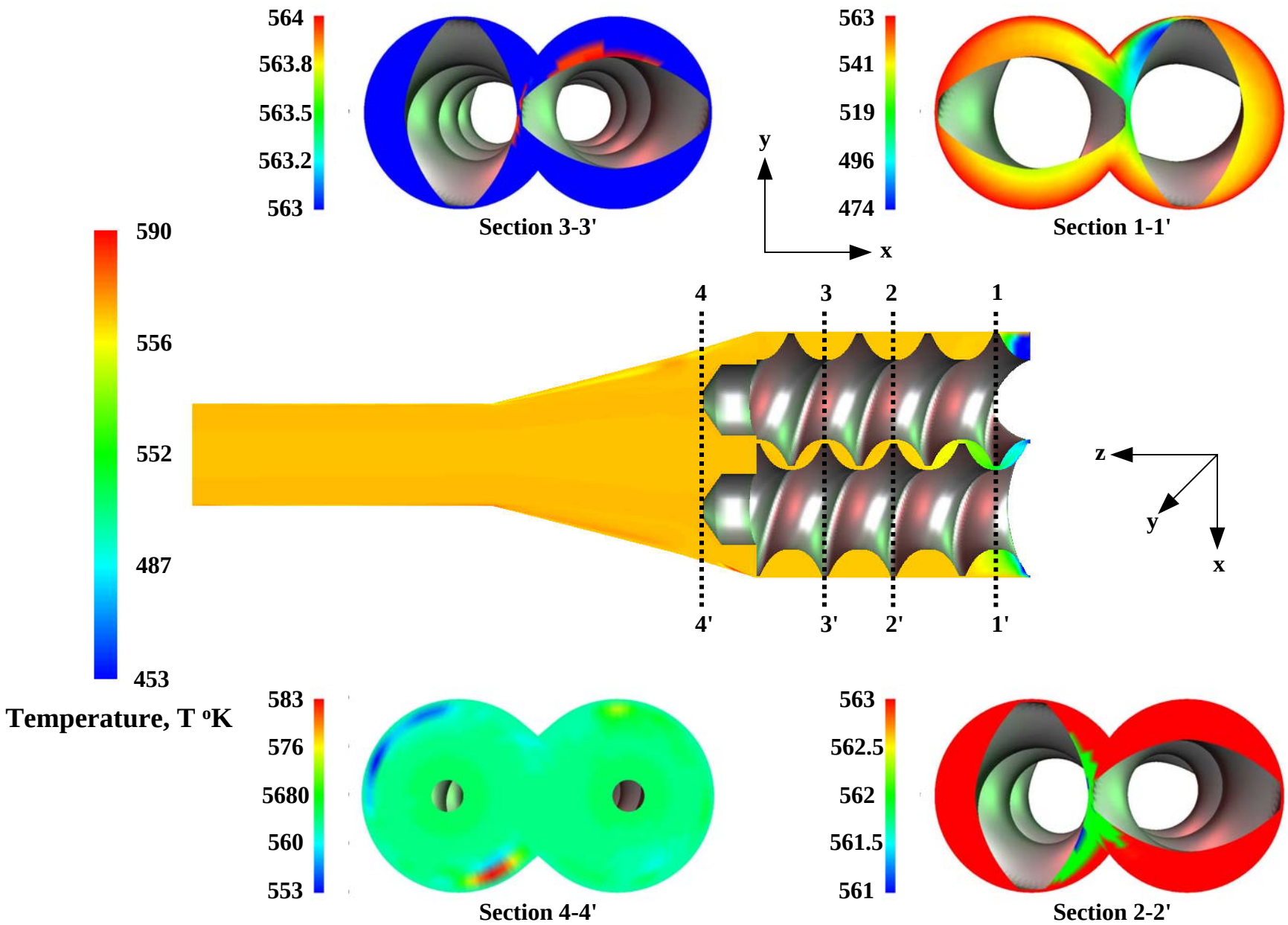
564
563.8
563.5
563.2
563
Section 3-3'
563
541
519
496
474
Section 1-1'
y
x
590
556
552
487
453
Temperature, T °K
4
3
2
1
4'
3'
2'
1'
z
y
x
583
576
5680
560
553
Section 4-4'
563
562.5
562
561.5
561
Section 2-2'

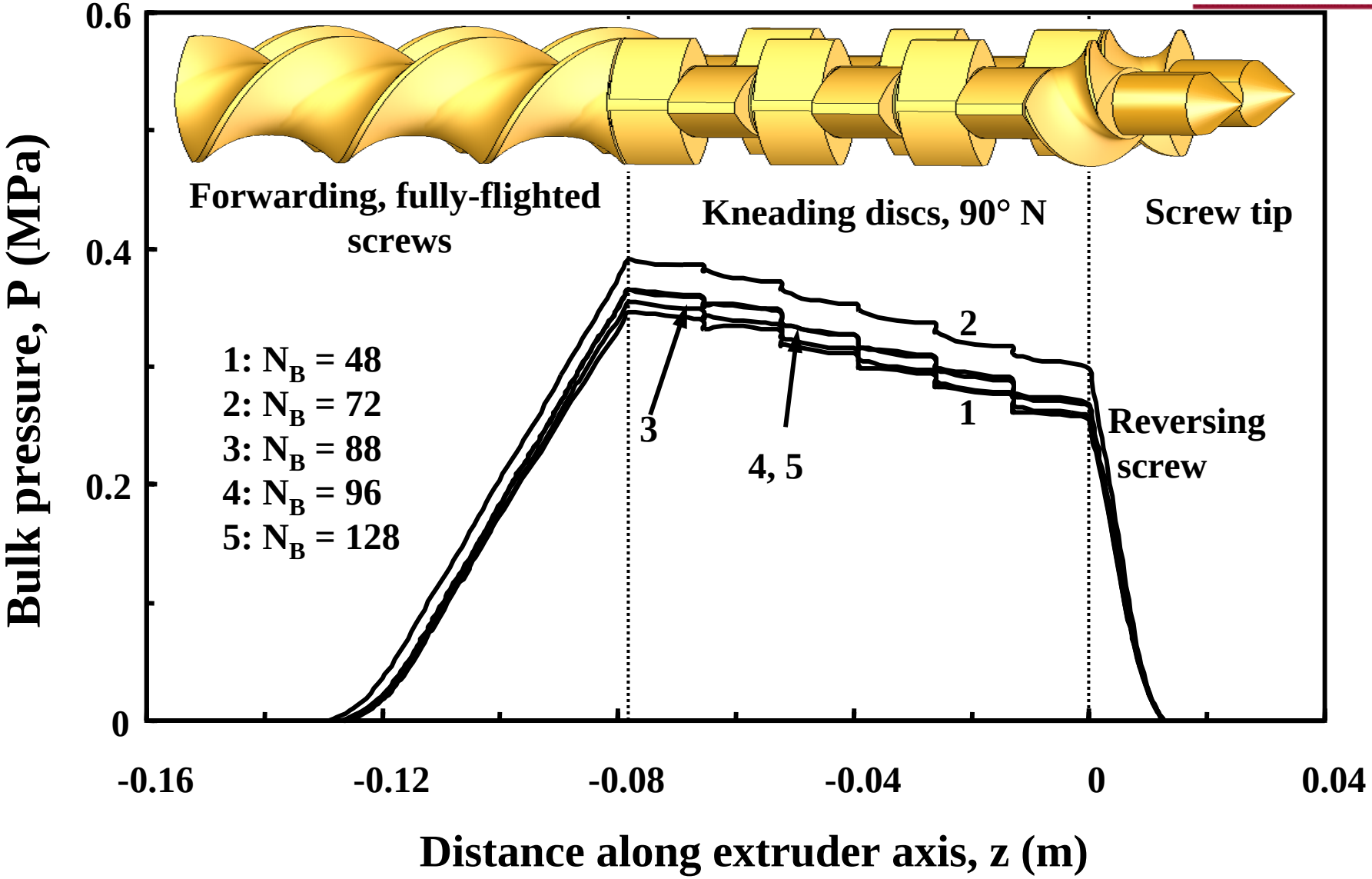
0.6
0.4
0.2
0
Bulk pressure, P (MPa)
Forwarding, fully-flighted screws
Kneading discs, 90° N
Screw tip
1: N_B = 48
2: N_B = 72
3: N_B = 88
4: N_B = 96
5: N_B = 128
2
1
3
4, 5
Reversing screw
-0.16
-0.12
-0.08
-0.04
0
0.04
Distance along extruder axis, z (m)

Fig. 37

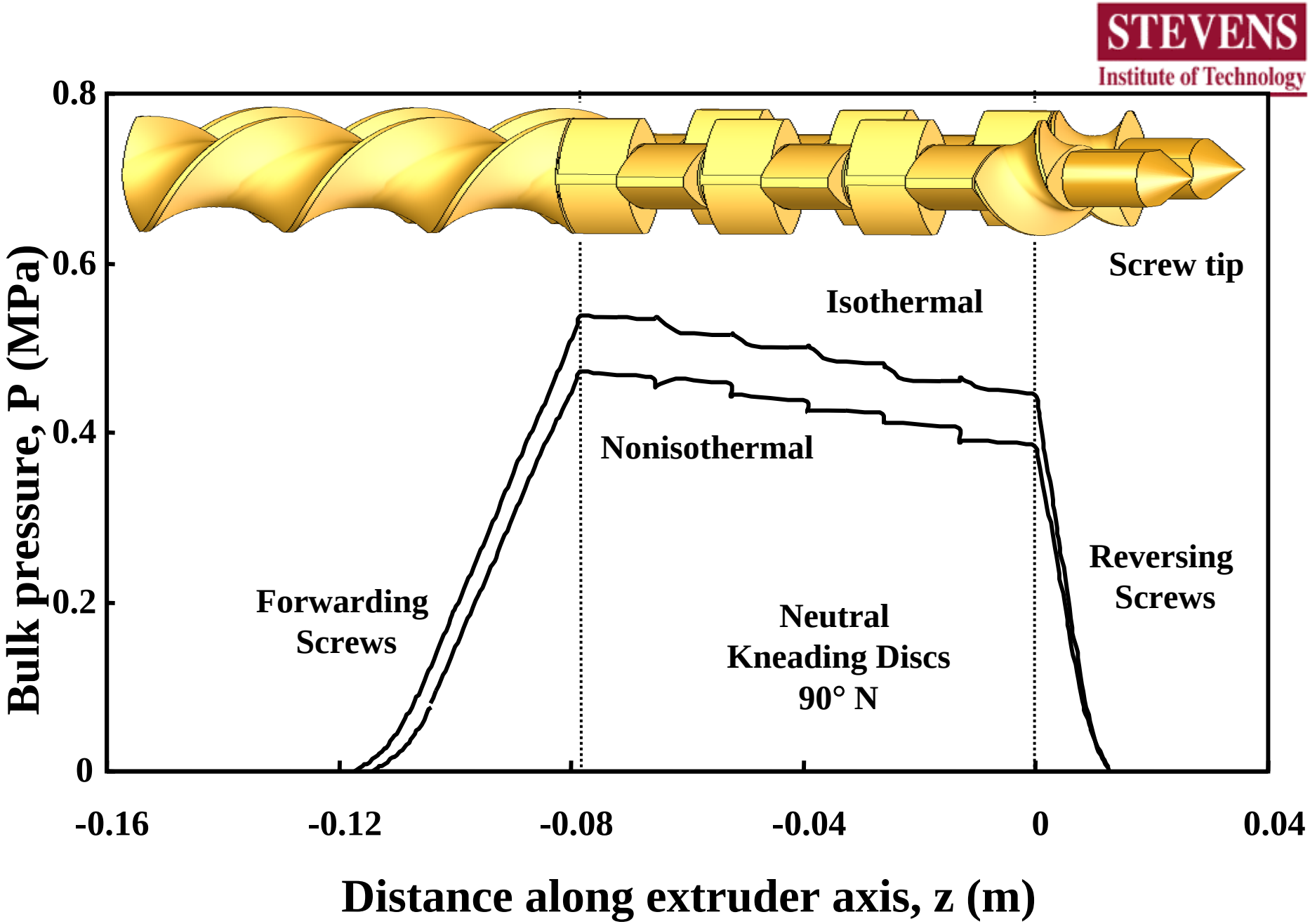
STEVENS
Institute of Technology
0.8
0.6
0.4
0.2
0
Bulk pressure, P (MPa)
Screw tip
Isothermal
Nonisothermal
Reversing
Screws
Forwarding
Screws
Neutral
Kneading Discs
90° N
-0.16
-0.12
-0.08
-0.04
0
0.04
Distance along extruder axis, z (m)

Fig. 38

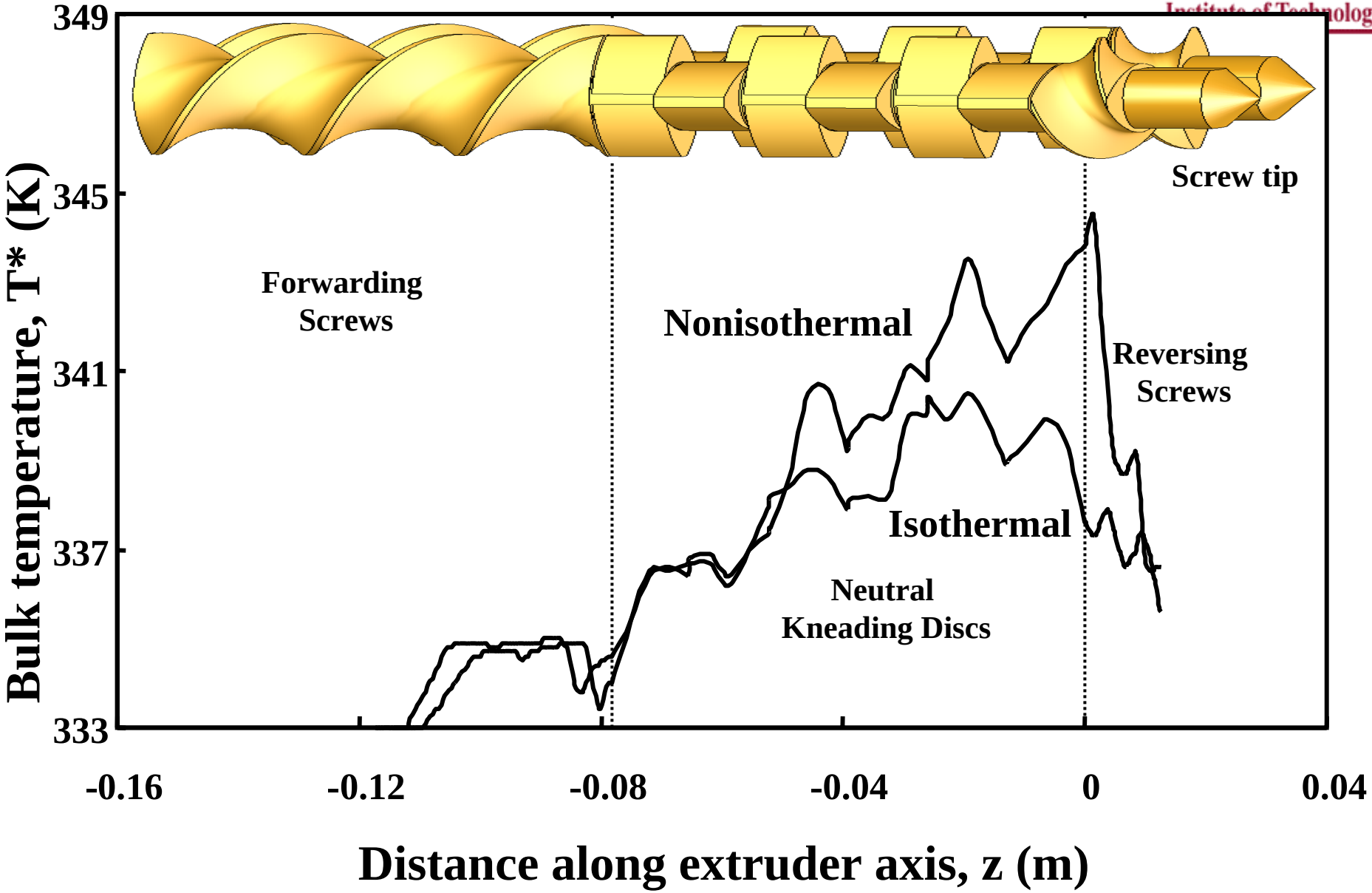
349
345
341
337
333
Bulk temperature, T* (K)
Forwarding
Screws
Nonisothermal
Isothermal
Neutral
Kneading Discs
Reversing
Screws
Screw tip
-0.16
-0.12
-0.08
-0.04
0
0.04
Distance along extruder axis, z (m)

Fig. 39

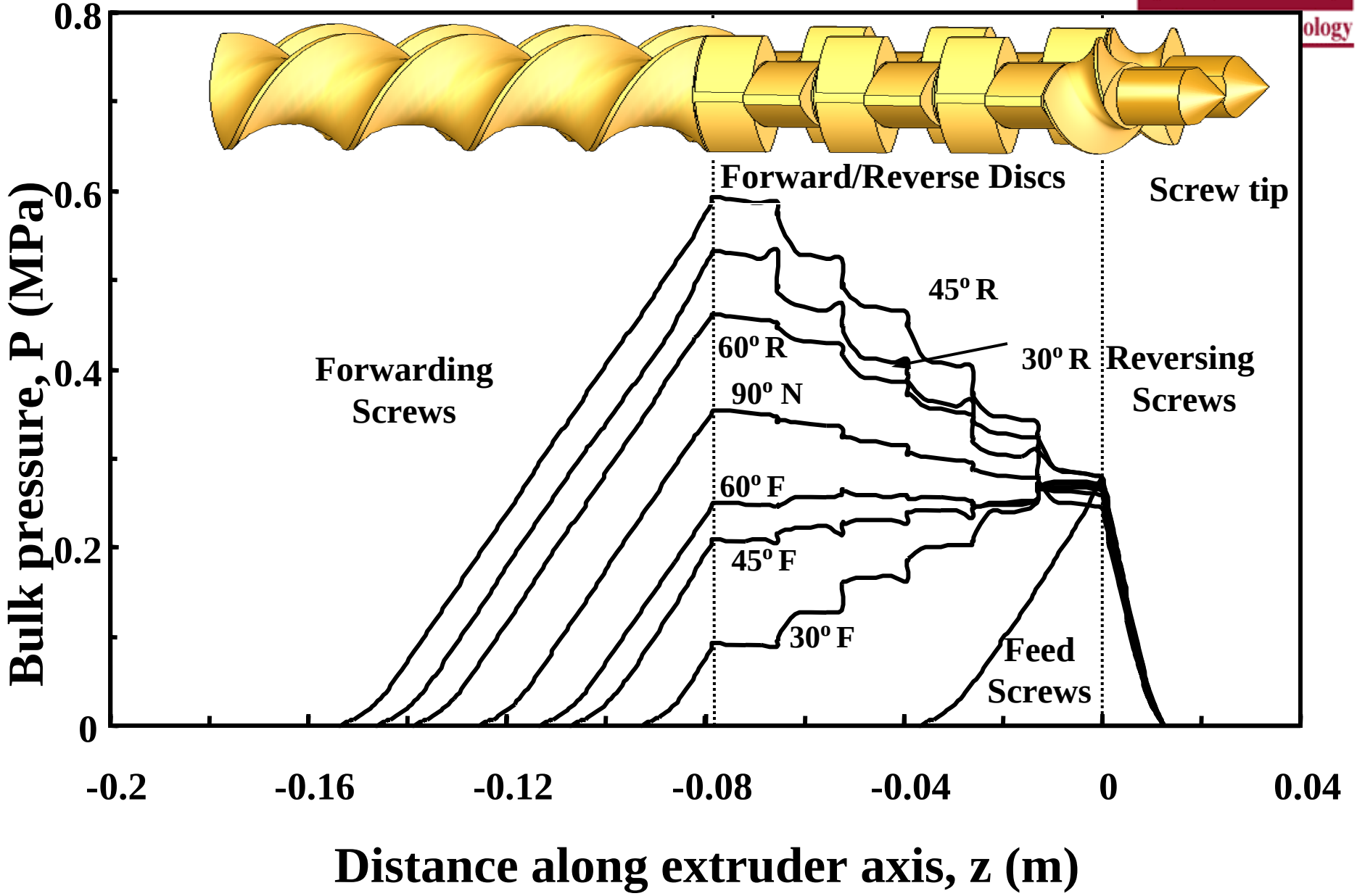
0.8
0.6
0.4
0.2
0
Bulk pressure, P (MPa)
-0.2
-0.16
-0.12
-0.08
-0.04
0
0.04
Distance along extruder axis, z (m)
Forward/Reverse Discs
Screw tip
45º R
60º R
30º R
Reversing Screws
Forwarding Screws
90º N
60º F
45º F
30º F
Feed Screws

Fig. 40

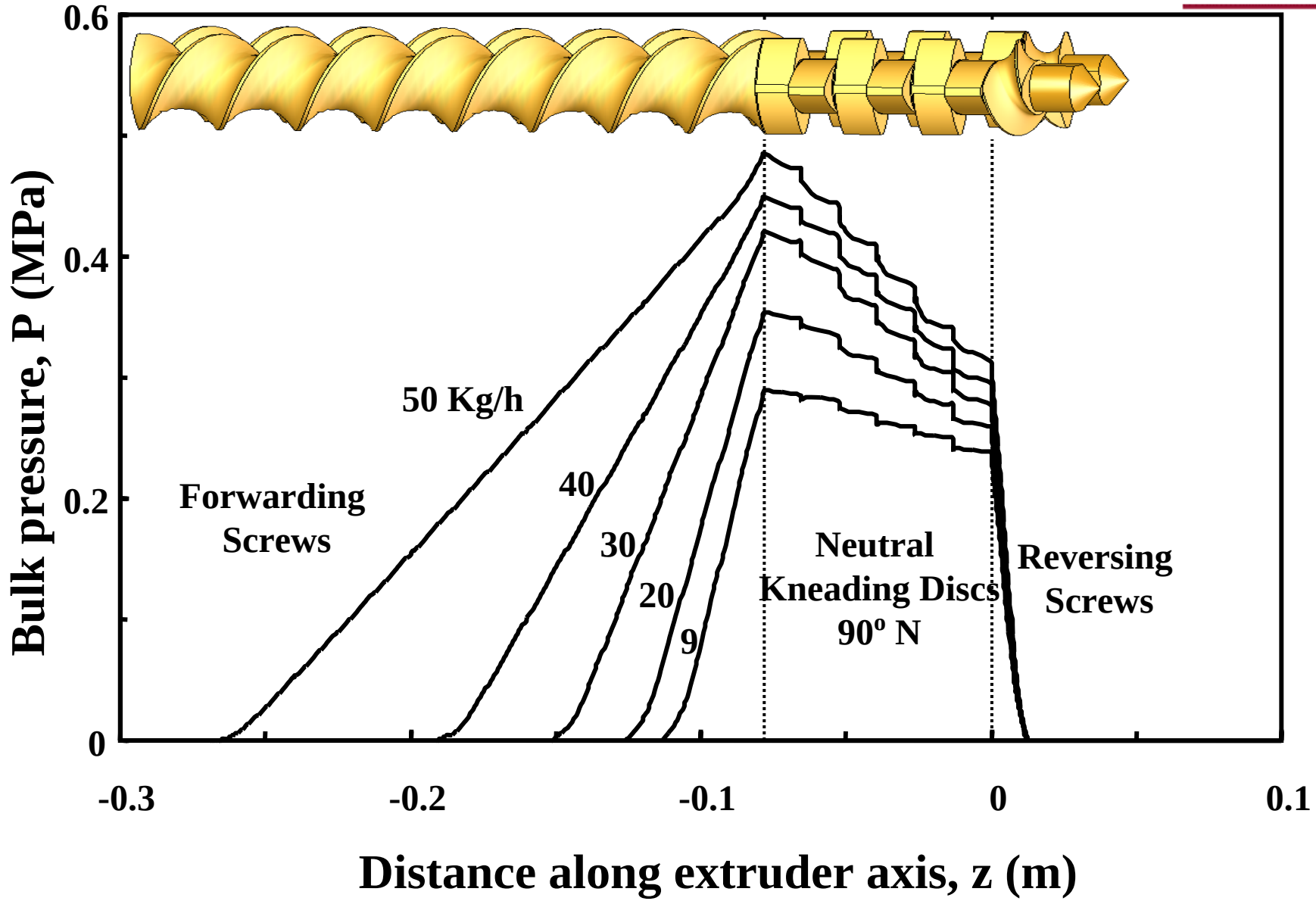
0.6
0.4
0.2
0
Bulk pressure, P (MPa)
50 Kg/h
40
30
20
9
Forwarding
Screws
Neutral
Kneading Discs
90º N
Reversing
Screws
-0.3
-0.2
-0.1
0
0.1
Distance along extruder axis, z (m)

Fig. 41

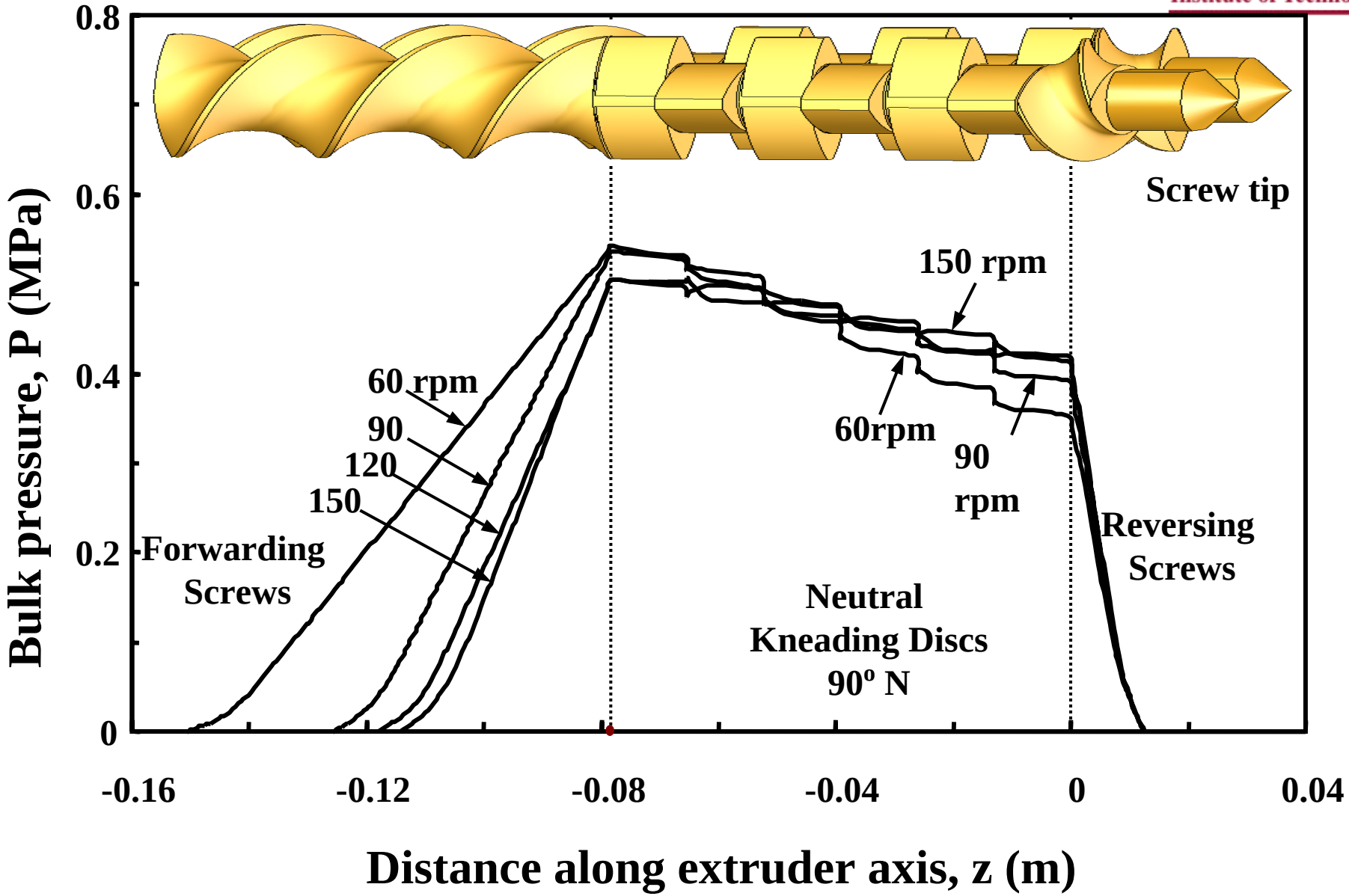
0.8
0.6
0.4
0.2
0
Bulk pressure, P (MPa)
-0.16
-0.12
-0.08
-0.04
0
0.04
Distance along extruder axis, z (m)
Screw tip
150 rpm
60 rpm
90
120
150
60rpm
90
rpm
Forwarding
Screws
Reversing
Screws
Neutral
Kneading Discs
90º N

Fig. 42

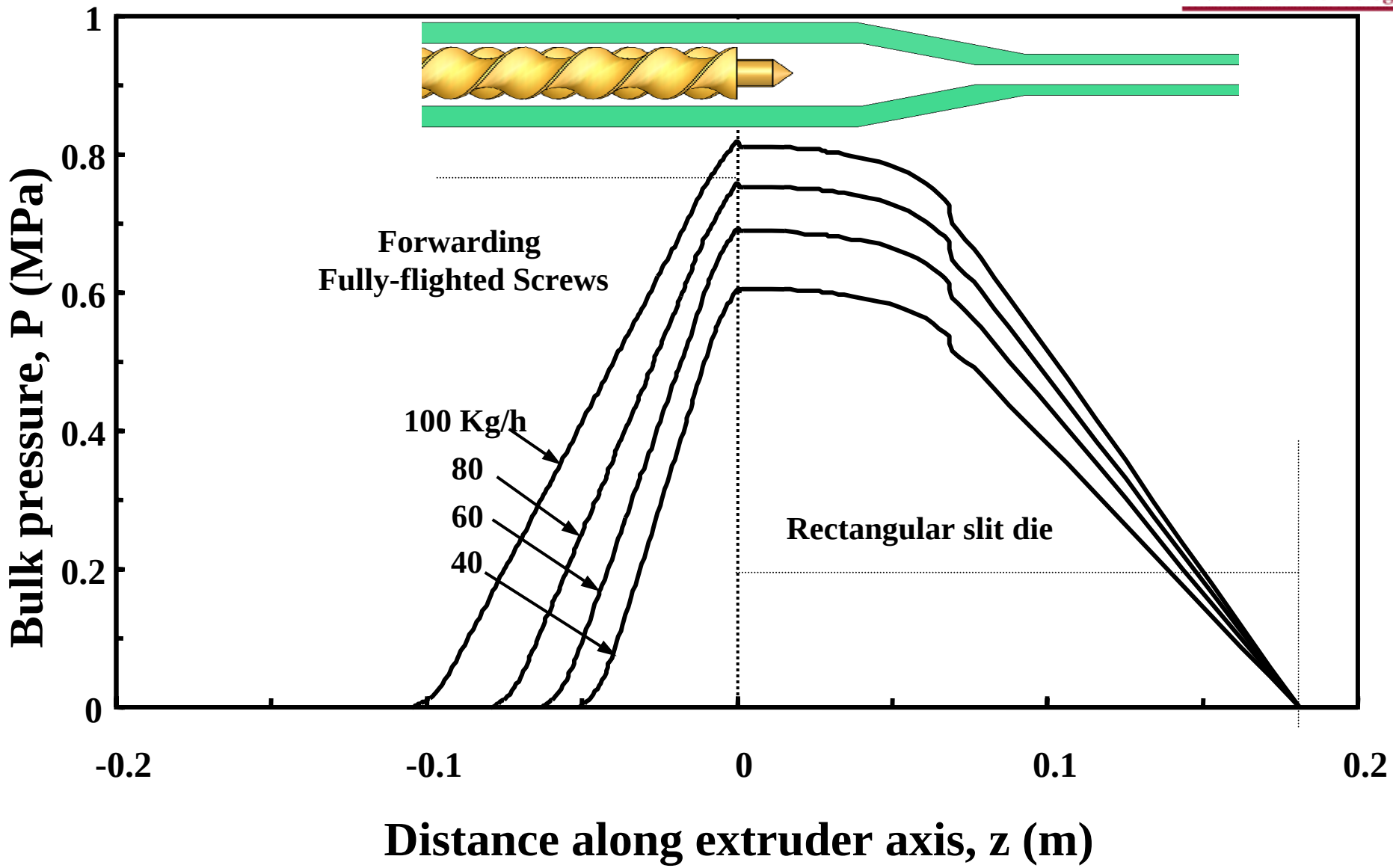
Bulk pressure, P (MPa)
1
0.8
0.6
0.4
0.2
0
-0.2
-0.1
0
0.1
0.2
Distance along extruder axis, z (m)
Forwarding
Fully-flighted Screws
100 Kg/h
80
60
40
Rectangular slit die

Fig. 43

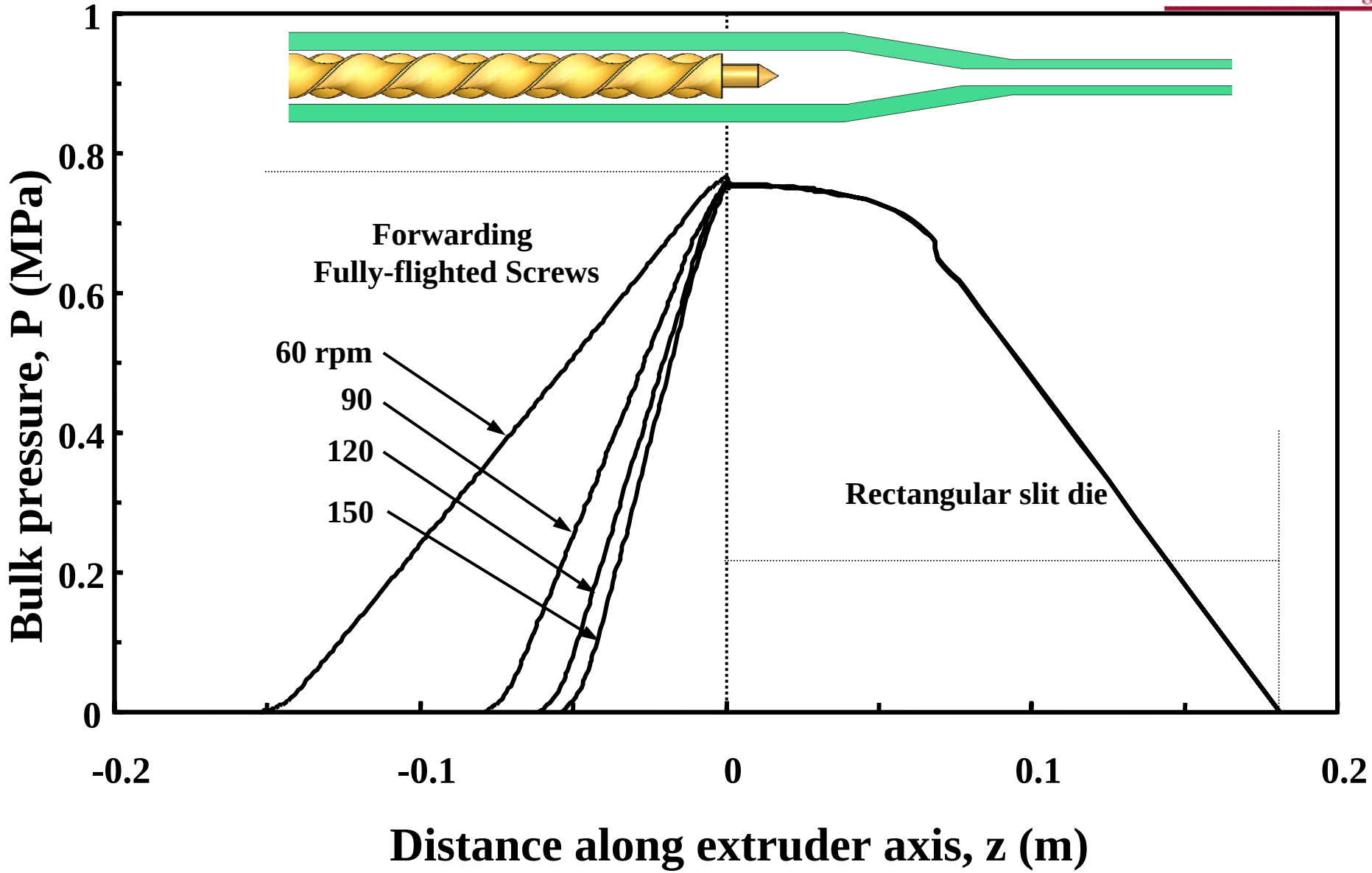
Bulk pressure, P (MPa)
1
0.8
0.6
0.4
0.2
0
-0.2
-0.1
0
0.1
0.2
Distance along extruder axis, z (m)
Forwarding
Fully-flighted Screws
60 rpm
90
120
150
Rectangular slit die

Fig. 44

STEVENS Institute of Technology

The benefit of this approach:

- Such work, done prior to the actual continuous processing of the live materials, eliminates or minimizes the subsequent risk associated with the precarious trial and error procedures and experimental studies that are prevalent in other industries.
- For other concentrated suspensions significant benefits at large flow rates or for high raw material/product costs

Fig. 45